Southeastern Geology: Volume 29, No. 2 December 1988

Edited by: S. Duncan Heron, Jr.

Abstract

Academic journal published quarterly by the Department of Geology, Duke University.

SOUTHEASTERN GEOLOGY

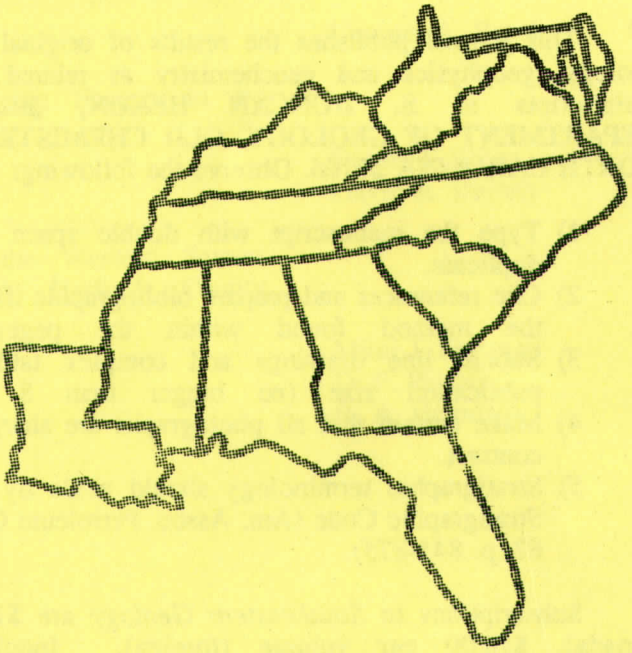

PUBLISHED AT DUKE UNIVERSITY DURHAM, NORTH CAROLINA

VOL. 29, NO. 2 DECEMBER 1988

SOUTHEASTERN GEOLOGY

PUBLISHED QUARTERLY

AT

DUKE UNIVERSITY

Editor in Chief:
S. Duncan Heron, Jr.

Managing Editor:
James W. Clarke

This journal publishes the results of original research on all phases of geology, geophysics and geochemistry as related to the Southeast. Send manuscripts to **S. DUNCAN HERON, JR., DUKE UNIVERSITY, DEPARTMENT OF GEOLOGY, OLD CHEMISTRY BUILDING, DURHAM, NORTH CAROLINA 27706**. Observe the following:

1) Type the manuscript with double space lines and submit in duplicate.
2) Cite references and prepare bibliographic lists in accordance with the method found within the pages of this journal.
3) Submit line drawings and complex tables reduced to final publication size (no bigger than 8 x 5 1/8 inches).
4) Make certain that all photographs are sharp, clear, and of good contrast.
5) Stratigraphic terminology should abide by the North American Stratigraphic Code (Am. Assoc. Petroleum Geologists Bulletin, v. 67, p. 841-875).

Subscriptions to *Southeastern Geology* are $12.00 per volume (US and Canada), $16.00 per volume (foreign). Inquires should be sent to: **SOUTHEASTERN GEOLOGY, DUKE UNIVERSITY, DEPARTMENT OF GEOLOGY, OLD CHEMISTRY BUILDING, DURHAM, NORTH CAROLINA 27706**. Make checks payable to: *Southeastern Geology*.

SOUTHEASTERN GEOLOGY

Table of Contents

Vol. 29, No. 2

December 1988

HYDROGEOLOGICAL FACTORS INFLUENCING WELL PRODUCTIVITY IN THE CRYSTALLINE ROCK REGIONS OF GEORGIA

GEORGE A. BROOK *Department of Geography, University of Georgia, Athens, GA 30602*

ABSTRACT

Data on 257 wells in the Georgia Blue Ridge and Piedmont provinces revealed that well productivity (PROD) was not related to bedrock lithology but did decrease significantly ($R^2 = 0.34$) with increasing well depth (DEPTH). The detailed study of 29 wells demonstrated that well productivity was determined both by well depth and by the distance between the well and a fracture trace intersection (DISTIN) mapped on aerial photographs. The relationship:

$$\log_e (PROD) = 5.08 - 0.00132 (5 \times DEPTH + DISTIN)$$

62 explained 81% of the variation in well productivity. This model suggests that, per foot of change, DEPTH has 5 times the effect on well productivity as DISTIN. However, because the range in DISTIN values was 5 times the range in DEPTH values, these two variables appeared to have an approximately equal effect on well productivity in the areas examined. The model indicates that to increase the likelihood of a high yield, and to reduce the depth and therefore the cost of obtaining a desired water supply, wells excavated in the crystalline rocks of Georgia should be located as close as possible to a fracture trace intersection visible on aerial photographs.

INTRODUCTION

The focus of future metropolitan and industrial development in Georgia will be in the Piedmont and Lower Blue Ridge regions—more specifically in the Atlanta and Athens-Gainesville areas. Unfortunately, the crystalline rocks in these areas do not provide significant quantities of ground water—typical wells producing 12-15 gpm up to 100 gpm. As a consequence, most water used by municipalities and industries is from surface water sources and because most streams are relatively small—with flows often below 1,000 cfs during dry weather periods—they are not always a reliable source of water (Ledbetter and Herwig, 1979). Growth of population in the Piedmont and Blue Ridge provinces will almost certainly require greater amounts of water than are available in the surface water system. Diversion of water from one river basin to another is a possible solution for specific problems but such transfers create water supply and water quality problems in the basins losing water. A more satisfactory solution would be the development of reliable and substantial ground water supplies.

Unfortunately, in crystalline rocks many wells fail to encounter water or have extremely low yields (Davis and Turk, 1964; Welby and Wilson, 1982 p. 86). Difficulties stem from the fact that the water-bearing and water-yielding properties of crystalline rocks depend on the number, depth, size, and degree of interconnection of the fractures (Summers, 1972). Heath (1979) has argued that if large supplies of ground water are to be obtained from the Piedmont and Mountain

regions well location must be selected with almost the same care as is used in selecting a dam site. Heath suggests that an average yield of 150 gpm might be obtained if well sites are chosen carefully. Confirming this are data presented by Cederstrom (1972). In a study of wells in the Piedmont and Mountain regions extending from Virginia to Maine Cederstrom found that yields of 100-300 gpm were common where efforts were made to obtain maximum yields. Although there is clear evidence that careful location of wells can increase yields substantially (Harman and others, 1984), in Georgia thorough studies of potential well sites are rarely carried out. In a study of 1,051 high-yielding (>20 gpm) wells in the greater Atlanta region of the Georgia Piedmont, Cressler and others (1983) found that most wells were located for the convenience of the users, and that the high yields had resulted largely by chance.

If ground water is to provide an increasing percentage of the future water needs of the Georgia Lower Blue Ridge and Piedmont regions, additional information is needed on the factors that influence well productivity so that high-yielding well sites can be located more easily and the potential productivity of a site can be estimated before drilling begins. The work of Mundorff (1948), LeGrand and Mundorff (1952) and LeGrand (1967) has suggested one possible way of increasing well yields. Using data for 802 wells in the Greensboro area and 490 wells in the Charlotte area of North Carolina, Mundorff (1948) and LeGrand and Mundorff (1952), found that average yields in gallons per minute per foot of well depth (gpm/ft) varied with topographic location. In the Greensboro area, average yields of wells located on hills, flats, slopes, draws, and valleys were 0.052, 0.113, 0.108, 0.148 and 0.132 gpm/ft, respectively; in the Charlotte area the yields of wells in these same locations were 0.072, 0.094, 0.111, 0.158, and 0.107 gpm/ft. In both areas hill locations provided the lowest yields and draws the highest. Utilizing these findings LeGrand (1967) developed a system whereby points are assigned to topographic locations based on their potential to provide ground water. LeGrand (1967) defined ten topographic categories with point values ranging from zero for a steep ridge (the least favorable situation) to eighteen for a draw in a large catchment area (the most favorable situation).

LeGrand's point value system is based on two assumptions. The first is that topography and ground water occurrence in crystalline rocks are both related to structural weaknesses. Hills and ridges are thought to be resistant because they are not heavily jointed and so the rock beneath them cannot contain substantial quantities of ground water. Valleys and draws, on the other hand, mark locations where structural weaknesses have been exploited by weathering and stream erosion. As the rocks beneath valleys and draws may have numerous openings, water should be more abundant in these locations. Mundorff (1948) considers draws to be better sites for high-yielding wells than valleys because, being narrow, they more exactly mark the locations of structural weaknesses. Valleys are often wide so that wells drilled in valley floors may not encounter the narrow zone of structural weakness along which the valley originally developed. The second assumption of LeGrand's point value system is that valleys and draws are better sites for high-yielding wells because the ground water table is closer to the surface than beneath hills and because the natural flow of water is away from wells in hills and ridges and towards wells in valleys and draws. This means that water can be obtained at shallower depth beneath valleys and draws and that there is a more rapid

and more reliable recharge to wells located in these environments.

The LeGrand point value system can be of considerable help in increasing average well yields. However, because valleys and draws are not always structurally controlled, it cannot be used to define exactly the locations and extents of the fracture zones that are the most reliable sources of ground water. Therefore, in recent years, researchers have attempted to map bedrock fracture zones directly. These zones are frequently visible as natural linear features on aerial photographs and can often be detected through considerable thicknesses of unconsolidated surface deposits. In this paper these linears seen on aerial photographs will be referred to as "fracture traces" following Lattman (1958), Lattman and Nickelson (1958), and Parizek (1976). They may or may not have a significant topographic expression. If, as the work of Mundorff and LeGrand implies, ground water in Piedmont rocks is concentrated in zones of fractured rock, knowledge of the exact locations of these zones should be useful in assessing the best locations for high-yielding wells.

This study uses fracture-trace-mapping techniques. It attempts to assess the influence of bedrock lithology and fracture characteristics on well productivity and to develop quantitative models that can be used to calculate, within reasonable limits, possible well productivities based on site characteristics. A principal aim of the research is to provide data that may be useful in locating sites for high-yield, high-productivity wells.

DATA COLLECTION

The yield of a well may be expressed in terms of its specific capacity which is defined as the yield in gpm/ft of drawdown for a stated pumping period. The specific capacity is affected predominantly by the hydraulic properties of the aquifer but also by the pumping period and the depth of saturated rock penetrated by the open section of the well bore. In order to compare well yields, specific capacity data must be adjusted to a common pumping period, and then divided by the depth of saturated rock penetrated by the open section of the well bore to give a productivity value in gpm/ft drawdown/ft of saturated rock penetrated.

In order to examine the geological factors influencing well productivity in the crystalline rock areas of Georgia data for 257 wells distributed throughout the Upper Blue Ridge, Lower Blue Ridge, and Piedmont provinces were obtained from Georgia Geological Survey files (Figure 1). Most of the wells were drilled by the Virginia Supply and Well Company of Atlanta, specific capacities were estimated from drawdown data at the end of a 24 hr pumping test. As water levels in most north Georgia wells stabilize during the first few hours of a pumping test (Charles Cressler pers. comm. 1984; Cressler and others, 1983) no standardization of well specific capacity for pumping period was considered necessary. Specific capacity data for the 257 wells were therefore considered suitable for statistical analysis and were corrected for the depth of saturated bedrock penetrated by the open section of the well bore to determine productivity values estimated in gpm per foot of drawdown per 1,000 feet of saturated bedrock penetrated (gpm/ft/10^3ft). The average yield of the 257 wells was 68 gpm (range 1.5-480), the average specific capacity was 0.77 gpm/ft (range 0.003-9.0), and the average productivity was 3.64 gpm/ft/10^3ft (range 0.005-42.8). Well depth ranged from 66-955 ft, the average

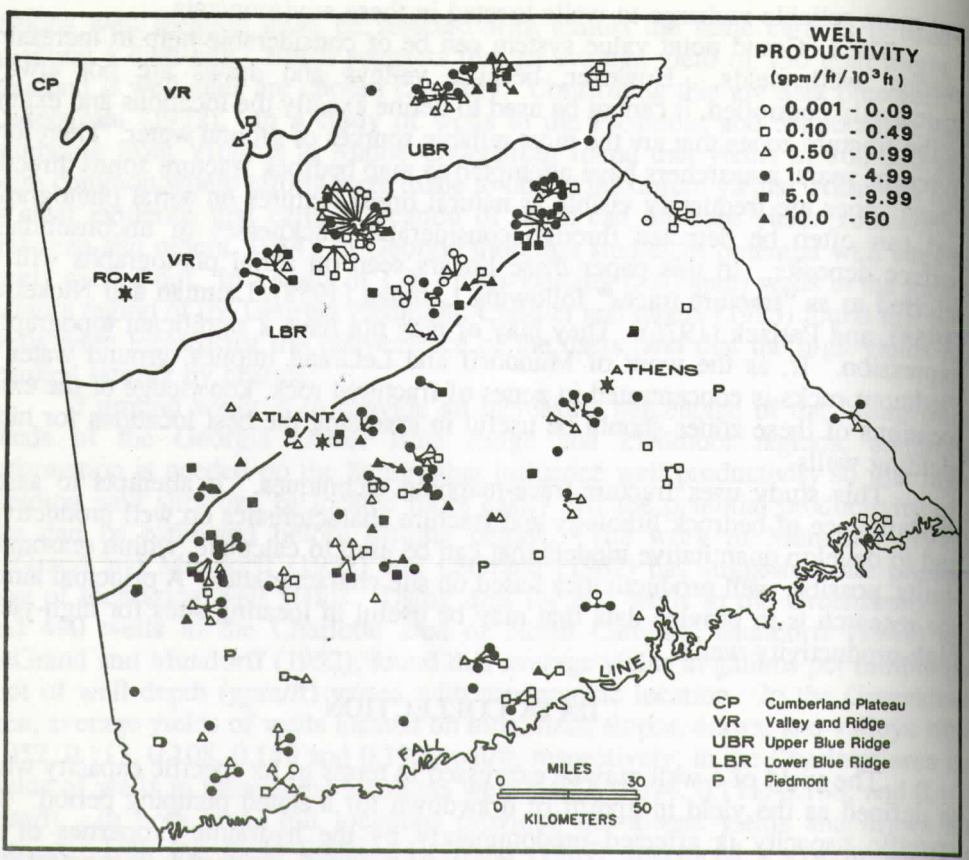

Figure 1. Topographic and geologic provinces of the study region and the locations and productivities of the 257 wells examined.

Table 1. Average production and depth characteristics of wells in different lithologies, Piedmont and Mountain regions, Georgia.

Rock Types*	Number of Wells	Yield[1] (gpm)	Specific Capacity[1] (gpm/ft)	Productivity[1] (gpm/ft/10^3 ft)	Depth[1] (ft)
A	8	39.5 (27.0)	0.33 (0.49)	1.46 (2.63)	480 (193)
B, C, D	118	74.1 (77.4)	0.73 (1.07)	3.19 (5.22)	435 (157)
E, G, H, K	102	60.4 (49.6)	0.81 (1.49)	4.35 (8.76)	392 (148)
J	5	52.8 (36.2)	0.31 (0.37)	1.21 (1.99)	553 (233)
L	14	90.1 (75.6)	0.96 (0.74)	4.31 (3.37)	305 (114)
M, N, O	10	72.9 (83.8)	1.26 (2.47)	4.12 (7.67)	342 (93)
A, B, C, D, L,	140	73.7 (75.5)	0.73 (1.02)	3.20 (4.97)	425 (160)
E, G, H, J, K	107	59.6 (49.2)	0.79 (1.46)	4.20 (8.58)	399 (155)
All	257	67.7 (66.3)	0.77 (1.29)	3.64 (6.79)	412 (157)

*A: granites, B: granite-gneiss, C: intermediate gneiss, D: biotite gneiss, E: metamorphosed mafic rocks, G: metagraywacke, H: mica schist, J: phyllitic rocks, K: aluminous schist, L: quartzite, M: cataclastic rocks, N: metavolcanic rocks, O: mafic and ultramafic rocks.

[1]Standard deviations are given in parentheses.

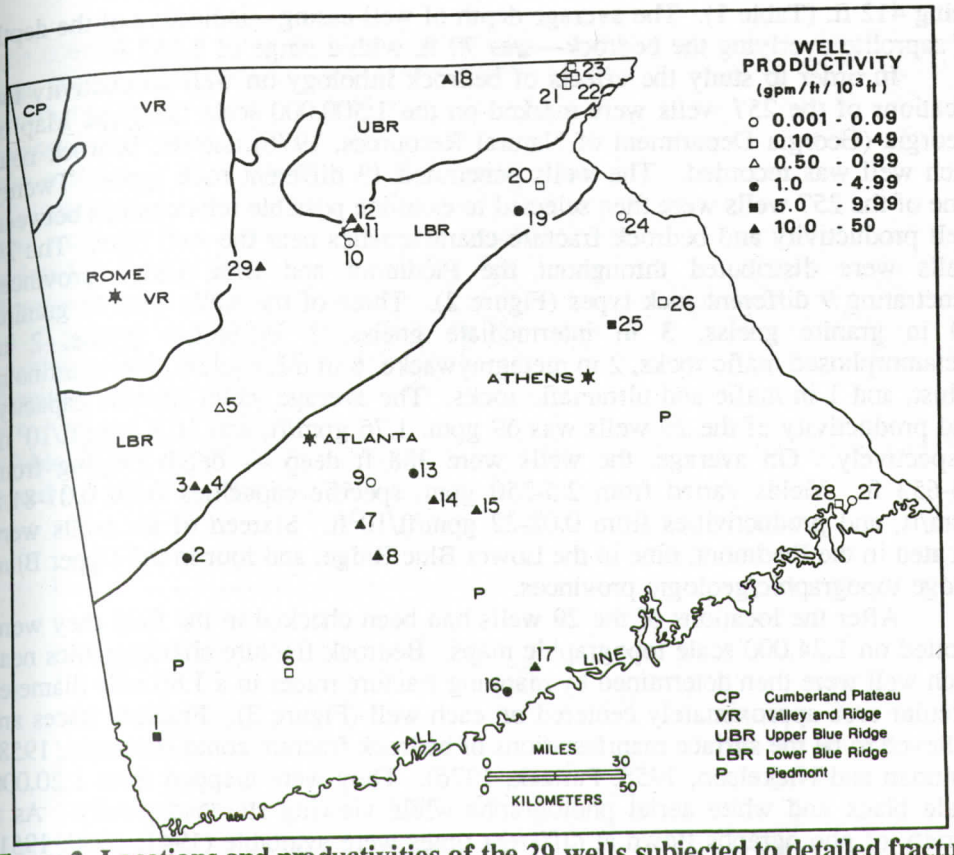

Figure 2. Locations and productivities of the 29 wells subjected to detailed fracture trace studies.

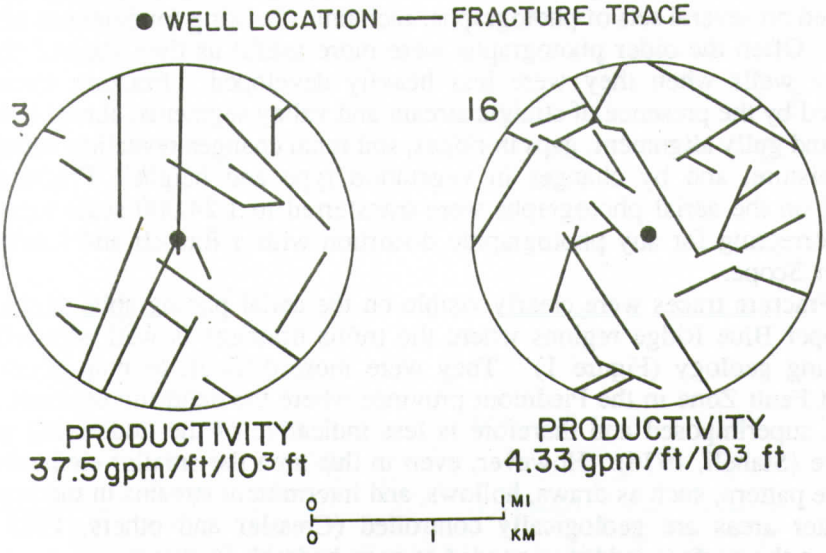

Figure 3. Fracture traces mapped in circular areas around wells 3 and 16 located in the Lower Blue Ridge and Piedmont provinces.

being 412 ft. (Table 1). The average depth of well casing—indicative of the depth of saprolite overlying the bedrock—was 70 ft. with a range of 8-212 ft.

In order to study the effects of bedrock lithology on well productivity the locations of the 257 wells were marked on the 1:500,000 scale Geologic Map of Georgia (Georgia Department of Natural Resources, 1976) and the bedrock near each well was recorded. The wells penetrated 13 different rock types. Twenty nine of the 257 wells were then selected to examine possible relationships between well productivity and bedrock fracture characteristics near the well bore. The 29 wells were distributed throughout the Piedmont and Blue Ridge provinces penetrating 9 different rock types (Figure 2). Three of the wells were in granite, 10 in granite gneiss, 3 in intermediate gneiss, 1 in biotite gneiss, 2 in metamorphosed mafic rocks, 2 in metagraywacke, 6 in mica schist, 1 in aluminous schist, and 1 in mafic and ultramafic rocks. The average yield, specific capacity, and productivity of the 29 wells was 69 gpm, 1.76 gpm/ft, and 10.3 gpm/ft/10^3 ft, respectively. On average, the wells were 388 ft deep — depth ranging from 66-653 ft. Yields varied from 2.5-250 gpm, specific capacities from 0.01-81.8 gpm/ft, and productivities from 0.02-22 gpm/ft/10^3ft. Sixteen of the wells were located in the Piedmont, nine in the Lower Blue Ridge, and four in the Upper Blue Ridge topographic/geologic provinces.

After the locations of the 29 wells had been checked in the field they were plotted on 1:24,000 scale topographic maps. Bedrock fracture characteristics near each well were then determined by mapping fracture traces in a 1.86 mile diameter circular area approximately centered on each well (Figure 3). Fracture traces are believed to be the surface manifestations of bedrock fracture zones (Lattman, 1958; Lattman and Nickelson, 1958; Parizek, 1976). They were mapped from 1:20,000 scale black and white aerial photographs while viewing stereoscopically. As a variety of photographs flown at different times were available (1941, 1950, 1951, 1955, 1958, 1960, 1963, 1964, 1966, 1967, 1971, 1972, and 1973), those showing fracture traces most clearly were used in the mapping. Most of the well sites were examined on several sets of photographs, each time checking for evidence of natural linears. Often the older photographs were more useful as they showed the areas near the wells when they were less heavily developed. Fracture traces were identified by the presence of straight stream and valley segments, abrupt changes in valley and gully alignment, gaps in ridges, soil tonal changes revealing variations in soil moisture, and by changes in vegetation type and height. Fracture traces mapped on the aerial photographs were transferred to 1:24,000 scale topographic maps correcting for any photographic distortion with a Bausch and Lomb Zoom Transfer Scope.

Fracture traces were clearly visible on the aerial photographs of the Lower and Upper Blue Ridge regions where the trellis drainage is well adjusted to the underlying geology (Figure 1). They were more difficult to map south of the Brevard Fault Zone in the Piedmont province where the dendritic drainage pattern may be superimposed and therefore is less indicative of the underlying geologic structure (Staheli, 1976). However, even in this area the smaller elements of the drainage pattern, such as draws, hollows, and intermittent streams in the uppermost headwater areas are geologically controlled (Cressler and others, 1983 p. 10) providing the surface evidence needed to map bedrock fractures.

It should be stressed that in many instances the fracture traces mapped during

the course of this study paralleled topographic lows such as valley and draw axes but that not all valleys and draws were mapped as bedrock fracture zones. Furthermore, soil tonal variations and vegetation patterns often revealed the presence of bedrock fracture zones having little or no topographic expression. In the early part of this study possible relationships between well productivity and distance to the nearest valley or draw axis were examined. This was done because the work of Mundorff and LeGrand suggested that well productivitiy might be related to the proximity of the well to a valley or draw — the productivity perhaps increasing with decreasing distance. There was such a low negative correlation (r = –0.3) between these two variables that this topographic factor was not considered further. Instead, the work concentrated on possible relationships between well location and fracture trace characteristics.

Table 2. Hydrogeological significance of water well and environmental variables used in multiple regression studies.

Variable Description	Variable Abbreviation	Hydrogeological Significance
Number of fracture traces (no/mi^2).	LINDEN	Estimates of the average secondary permeability in the bedrock around the well bore and the degree of integration of lines of secondary permeability. Ground water movement to the well bore should increase with increases in these variables
Number of fracture trace intersections (no/mi^2).	INTDEN	
Distance to the nearest fracture trace (ft)	DISTL	Estimates of the closeness of a well to possible zones of high secondary permeability. Ground water flow to a well should increase with decreases in these variables.
Distance to the nearest fracture trace intersection (ft)	DISTIN	
Length of the closest fracture trace (ft)	LENTH	Estimate of the magnitude of ground water flow in the nearest zone of high secondary permeability. Ground water flow to a well should increase with an increase in this variable.
Depth of the well (ft)	DEPTH	Estimate of the frequency and openness of fractures encountered by the well bore. Ground water flow to the well bore per foot of well should decrease with an increase in this variable.

Five fracture trace properties were measured in the circular sample areas around the 29 wells. These variables and their possible hydrogeologic significance are listed in Table 2. The number of fracture traces (LINDEN) and the number of fracture trace intersections (INTDEN) are measures of the average secondary permeability of the crystalline rock aquifer and therefore of the magnitude of ground water flow to be expected in the region around the well. As these variables increase, well productivities in the general area might be expected

to increase. In the regions near the 29 wells LINDEN varied from 2.2 to 22 per square mile and INTDEN from 0.4 to 11.3 per square mile (Table 3). The distances between a well and the nearest fracture trace (DISTL) and the nearest fracture trace intersection (DISTIN) are measures of the proximity of the well to possible localized zones of higher aquifer permeability. Wells on or close to such zones should have higher productivities. Three of the 29 wells were located on fracture traces and one was on a fracture trace intersection. The maximum distance between a well and a fracture trace was 1,167 ft and the maximum distance to a fracture trace intersection was 3,067 ft. Ground water flow to a well bore is also likely to increase with an increase in the length of the nearest fracture trace (LENTH). This is because fracture zones of considerable horizontal extent are likely to be the more important ground water flow paths. For the 29 wells the length of the closest fracture trace varied from 500 ft to 10,266 ft (Table 3).

Table 3. Data on the 29 wells subjected to detailed fracture trace analysis.

WELL[1] ID	YIELD (gpm)	SPECIFIC CAPACITY (gpm/ft)	PRODUCTIVITY (gpm/ft/10^3 ft)	LINDEN (no/mi^2)	INTDEN (no/mi^2)	DISTL (ft)	DISTIN (ft)	LENTH (ft)	DEPTH (ft)	ROCK TYPE*
1	60.0	1.50	7.85	6.2	6.2	33	1233	2067	225	A
2	18.0	0.30	2.61	9.5	2.2	233	1100	1067	231	B
3	60.0	6.00	37.50	7.7	2.6	0	0	10266	200	H
4	48.0	4.36	31.37	11.3	4.0	100	1300	2067	158	H
5	41.0	0.34	0.95	9.2	2.2	1167	1867	1233	450	B
6	25.0	0.14	0.29	7.0	2.2	1000	1767	4233	500	H
7	34.0	0.60	30.00	7.3	4.0	800	1000	3267	66	C
8	40.0	1.80	33.96	3.3	0.7	600	1706	5710	126	C
9	3.0	0.01	0.02	5.1	0.4	1000	2833	3800	500	A
10	9.8	0.05	0.09	20.9	7.3	460	933	1903	603	H
11	102.0	2.49	10.37	20.9	11.3	0	1167	4233	286	H
12	129.0	1.50	21.13	22.0	10.3	67	200	3333	146	H
13	133.0	1.16	2.09	4.0	0.4	400	1033	1333	600	B
14	45.0	3.00	14.29	8.4	3.7	133	400	500	240	B
15	67.0	6.70	18.31	8.1	2.2	200	767	1267	430	C
16	175.0	0.88	4.33	11.3	6.6	500	833	1933	230	D
17	250.0	6.25	34.34	3.3	0.4	100	459	1567	250	E
18	90.0	8.18	25.72	12.8	3.3	0	267	5333	362	O
19	108.0	0.43	1.02	12.8	3.7	67	733	2167	545	G
20	44.0	0.18	0.33	9.9	7.0	267	1667	1167	600	G
21	65.0	0.18	0.47	12.1	2.2	1033	2867	1067	445	B
22	16.0	0.07	0.20	12.1	2.2	1033	2867	1067	545	B
23	32.0	0.14	0.31	12.1	2.2	1033	2867	1067	605	B
24	7.5	0.04	0.07	5.5	1.1	1333	3067	1833	653	E
25	115.0	1.64	6.80	2.2	0.7	133	833	1733	300	K
26	47.8	0.10	0.19	14.3	2.6	700	1300	800	600	A
27	2.5	0.01	0.02	4.8	1.5	233	2767	1233	500	B
28	7.9	0.06	0.11	4.8	1.5	833	2867	1233	600	B
29	230.0	3.07	13.77	19.8	8.4	133	167	2167	253	B

[1] Variable abbbreviations are listed in Table 2.
*Rock type abbreviations are listed in the footnote to Table 1.

LITHOLOGY AND WELL PRODUCTIVITY

The possibility that well productivities were significantly higher in some lithologies than in others was examined using data for the 257 wells shown in Figure 1. Initially the 13 rock types in which the wells were located were collapsed into six broad lithologies by grouping rocks with generally similar hydrogeological properties. The six lithologies were: granites, gneisses (granite gneiss, intermediate gneiss, biotite gneiss) quartzites, phyllites, schists (metamorphosed mafic rocks, metagraywacke, mica schist, aluminous schist), and

a group consisting of cataclastic, metavolcanic, and mafic and ultramafic rocks. There were 8, 118, 102, 5, 14, and 10 wells, respectively, in these six lithologies (Table 1). Mean well productivities in each lithology were compared by conducting a T-test. Although group mean productivities varied from 1.21 gpm/ft/10^3 ft in phyllites to 4.35 gpm/ft/10^3 ft in schists, only wells in quartzites were found to have productivities significantly different from those in other rock types at the 0.1 probability level.

In a second analysis the 13 rock types were collapsed into two hydrogeologically similar groups—the first group including granites, gneisses, and quartzites, the second group consisting of schists and phyllites. Although the mean productivities of wells penetrating the rocks of these two groups were 3.20 and 4.20 gpm/ft/10^3ft., respectively, this difference was not significant at the 0.1 probability level (Table 1).

These results suggest that in the crystalline rock regions of Georgia well productivities do not vary significantly with lithology. Therefore, further analyses examined the possible roles of well depth and of well location with respect to bedrock fractures in determining well productivities.

THE INFLUENCE OF WELL DEPTH ON PRODUCTIVITY

Previous studies of water wells in crystalline rocks have demonstrated that measures of well production (e.g. yield, specific capacity) per foot of well decrease with increasing well depth. For example, from a study of 806 wells in the Greensboro area of North Carolina, Mundorff (1948) reported that the average yield of wells in gallons per minute per foot of well below the water table decreased with well depth from 0.222 gpm/ft for wells 0-100 feet deep to 0.091 gpm/ft for wells more than 300 feet deep. Summers (1972) found that the specific capacities of 56 wells tapping fractured crystalline rocks in Marathon County, Wisconsin were inversely related to the depth of the well. Davis and Turk (1964) studied records for 2,565 wells in crystalline rocks in the eastern U.S.A. and in the Sierra Nevada and examined data on 1,291 water pressure tests in 340 drill holes. They concluded that in crystalline rocks well yield in gpm per foot of well decreases rapidly with depth. A negative correlation between well depth and well yield/ft of well was also noted in Wake County, N. Carolina by Welby and Wilson (1982). According to Cressler and others (1983) well yield and specific capacity per foot of well decrease with increasing well depth because the fractures through which the water moves are less numerous and less open at increasing depth. As a result, the volume of water contained in the crystalline rock aquifer is less in the deeper parts of the rock mass than it is nearer the surface where open, interconnected fractures are more numerous.

Productivity-depth relationships were developed for the full data set of 257 wells and for the subset of 29 wells. These relationships:

$$\log_e (\text{PROD}) = 2.6497 - 0.006\ (\text{DEPTH}) \text{ ---- } (N = 257, R^2 = 0.34) \quad (1)$$

$$\log_e (\text{PROD}) = 5.0018 - 0.112\ (\text{DEPTH}) \text{ ---- } (N = 29, R^2 = 0.69) \quad (2)$$

were significant at the 0.0001 level and explained 34% and 64% of the variability in well productivity, respectively. These models indicate that in the crystalline rock areas of Georgia there is a statistically significant relationship between well productivity and well depth — with productivity decreasing as well depth in-

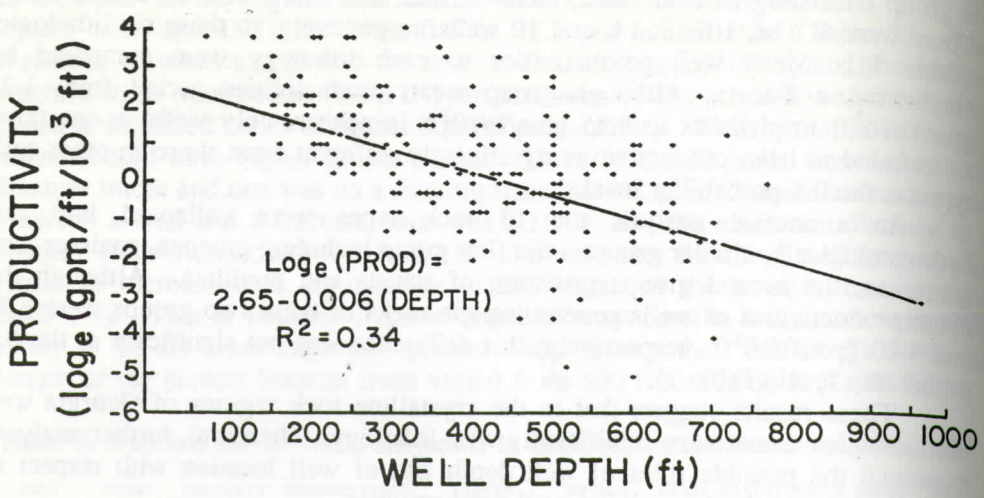

Figure 4. Relationship between well productivity and well depth for the data set of 257 wells.

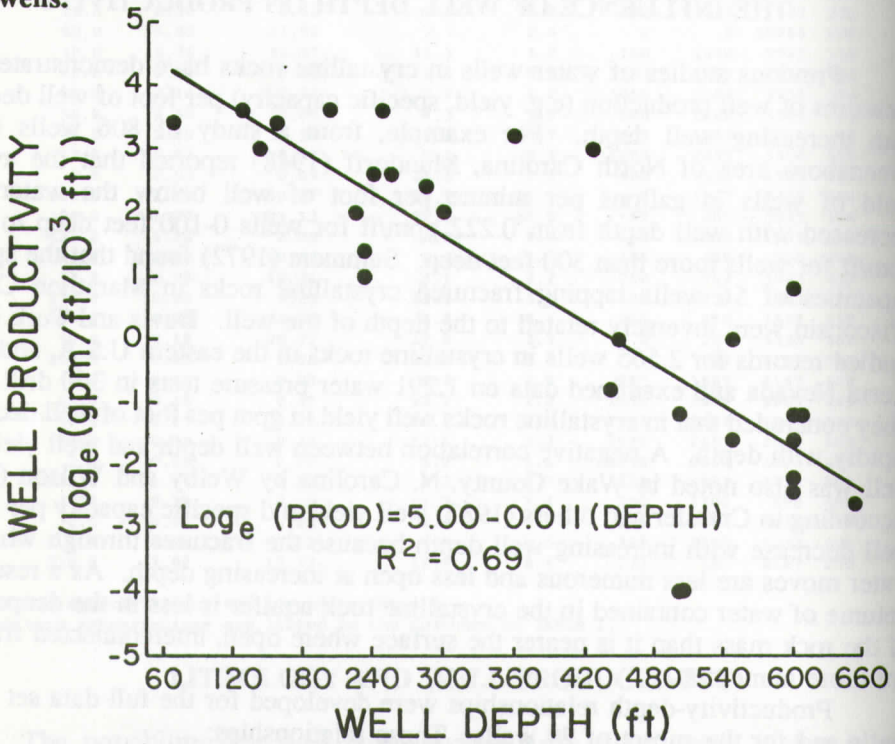

Figure 5. Relationship between well productivity and well depth for the 29 wells selected for fracture trace studies.

creases (Figures 4 and 5). The considerable scatter about both regression lines and the fact that different data sets give different models suggest that other factors — most likely well location factors — influence well productivity and possibly also well depth. This last possibility was examined first.

LOCATIONAL FACTORS AFFECTING WELL DEPTH

In an effort to determine if well location — in terms of proximity to bedrock fractures — influences well depth, possible relationships between depth and the fracture trace variables DISTIN, DISTL, LINDEN, INTDEN, and LENTH were investigated. Stepwise multiple linear regression analysis with DEPTH as the dependent variable revealed that the relationship:

DEPTH = 23.5 + 0.108 (DISTIN), (3)

which was significant at the 0.001 level, explained 34% of the variation in DEPTH (Figure 6). No other variables were significant at the 0.15 level.

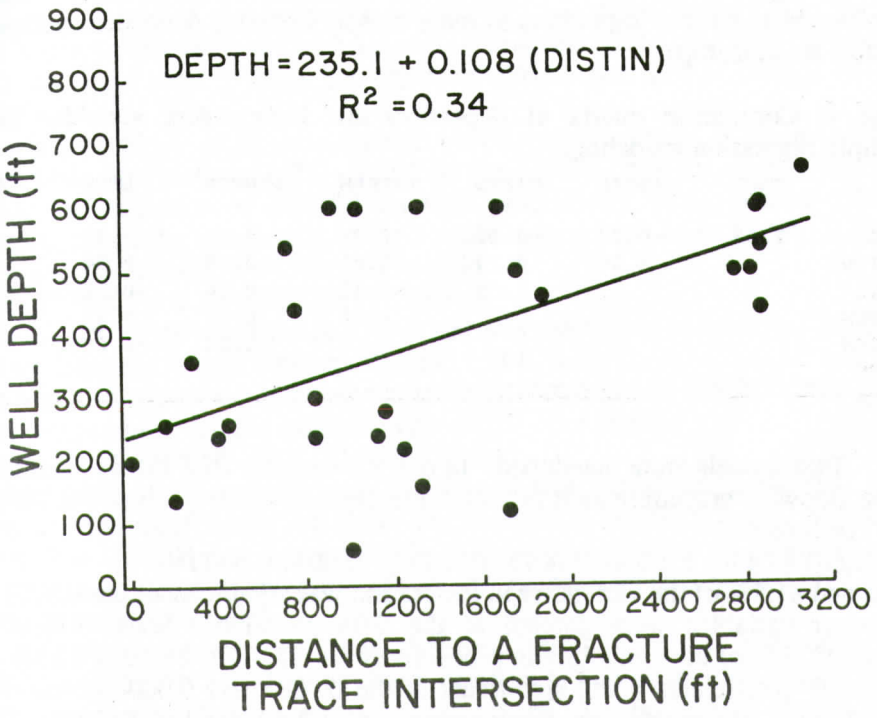

Figure 6. Relationship between well depth and distance to a fracture trace intersection.

This model indicates that well depth depends on well location — wells being deeper at increasing distance from a fracture trace intersection. The obvious conclusion to be drawn from this relationship is that when a well is drilled close to a fracture trace intersection a relatively shallow well produces the desired water supply. On the other hand, a well drilled at some distance from a fracture trace intersection does not produce an adequate water supply quickly and so the well is drilled to greater and greater depth until the needs of the user are satisfied. This finding is important because it indicates that many of the reported relationships between measures of well production per foot of well and well depth are misleading. These relationships can not be regarded as accurate quantitative estimates of the effect of well depth on well production. This is because the

variable well depth — highly correlated with DISTIN — incorporates the influences both of well location (e.g. DISTIN) and of well depth on well productivity. It is clear from this result that any predictive model of well productivity should include the effects both of well depth and well location. Multiple regression modeling was therefore attempted.

PREDICTING PRODUCTIVITY USING WELL DEPTH AND FRACTURE TRACE CHARACTERISTICS

Exploratory stepwise multiple linear regression analysis was undertaken with PROD as the dependent variable and with DISTIN, LINDEN, INTDEN, LENTH, and DEPTH as the independent variables. Well productivities were transformed to natural logarithms to more closely linearize dependent-independent variable relationships.

Table 4. Correlation matrix of dependent and independent variables used in multiple regression modeling.

	PROD	DISTIN	DISTL	INTDEN	LINDEN	LENTH	DEPTH
PROD	1.00	-0.77	-0.62	0.26	0.07	0.38	-0.83
DISTIN		1.00	0.78	-0.41	-0.29	-0.32	0.58
DISTL			1.00	-0.42	-0.20	-0.22	0.50
INTDEN				1.00	0.81	0.07	-0.28
LINDEN					1.00	-0.0005	-0.03
LENTH						1.00	-0.39
DEPTH							1.00

Two models were developed. In one the variable DEPTH was entered first in the stepwise procedure as it provided the greatest explanation of PROD (Table 4). The model:

$$\log_e(\text{PROD}) = 5.2294 - 0.0078\,(\text{DEPTH}) - 0.0011\,(\text{DISTIN}) \quad (4)$$

explained 81.5% of the variability in PROD and was significant at the 0.0001 level. No other variables were entered at the 0.05 probability level. Well depth explained 69% of the variability in productivity and DISTIN a further 12.5% — the respective coefficients being significant at the 0.0001 and 0.0003 levels. In the second model the greatest emphasis was given to the locational variable DISTIN. Although it provided slightly less explanation of PROD than did DEPTH ($r = -0.77$ compared to -0.83 for DEPTH, Table 4) it was entered first and other variables were regressed against the residuals. The model:

$$\log_e(\text{PROD}) = 5.4029 - 0.0019\,(\text{DISTIN}) - 0.0052\,(\text{DEPTH}) \quad (5)$$

explained 74% of the variability in productivity. No other variables were entered at the 0.05 probability level. DISTIN explained 59% of the variability in PROD and DEPTH explained an additional 15% — the respective regression coefficients were significant at the 0.0001 and 0.0006 levels.

The negative relationships in these models between productivity and DEPTH and between productivity and DISTIN suggest that in crystalline rocks water is held in fractures and that the number and openness of fractures declines with depth and with distance from a fracture zone. It is likely that well productivity is more highly correlated with DISTIN ($r = -0.77$) than with DISTL ($r =$

–0.62) because wells drilled above a fracture trace intersection draw water directly from two major bedrock fracture zones. By comparison wells drilled on a fracture trace but at some distance from a fracture trace intersection only draw water directly from one bedrock fracture zone.

Although both models provide a high degree of explanation of the variability in well productivity, neither provides an accurate estimate of the individual effect of either DEPTH or DISTIN on well productivity. This is because these two variables are reasonably highly correlated (r = 0.58) so that the variable entered into the regression first provides some explanation of well productivity that should be accounted for by the other variable. For both variables the regression coefficient was higher when the variable was entered first. Based on the ratios between the regression coefficients — approximately 7 in the first model and approximately 3 in the second — it seems likely that DEPTH has less than 7 but more than 3 times the effect on PROD per foot of change as does DISTIN.

As 7 of the 29 wells were located within a narrow range of distance from a fracture trace intersection (1,000 - 1,300 ft) these wells provided an opportunity to examine the influence of DEPTH on well productivity while holding DISTIN essentially constant. The depths of the 7 wells ranged from 66 to 600 ft (1, 2, 4, 7, 11, 13, and 26 in Table 3). The relationship:

$$\log_e(\text{PROD}) = 4.11 - 0.007257\ (\text{DEPTH}) \qquad (6)$$

explained 77% of the variation in PROD and was significant at the 0.004 level. As six of the 29 wells ranged between 225 and 253 ft. deep (1, 2, 14, 16, 17, and 29 in Table 3), these were used to assess the effect of variations in DISTIN (167 - 1,233 ft) on well productivity for constant well depth. The model:

$$\log_e(\text{PROD}) = 3.27 - 0.001514\ (\text{DISTIN}) \qquad (7)$$

explained 48% of the variability in PROD and was significant at the 0.13 level. The regression coefficients of these two equations (0.007257) and 0.001514) suggest that DEPTH has approximately 5 times more effect on productivity as DISTIN — a value lying mid-way between the ratios suggested by the two multiple regression models 4 and 5.

The regression results indicate that well PROD is strongly affected by both DEPTH and DISTIN and that the effect of depth is approximately 5 times that of DISTIN per foot of change. As well depth ranged from 66 - 653 ft (range 587 ft) and DISTIN ranged from 0 - 3,067 ft (range 3,067 ft) the range for DISTIN was approximately 5 times (actually 5.2 times) that of DEPTH. Thus, although DEPTH affects PROD 5 times as much as DISTIN per foot of change, the range of values involved is 5 times greater for DISTIN than for DEPTH. This means that the effect of DEPTH on PROD is approximately the same as the effect of DISTIN.

The evidence indicates that the two variables most useful in explaining and predicting well productivity are DEPTH and DISTIN and that a problem in using these variables in a multivariate model to predict PROD is that they are reasonably highly correlated (r = 0.58). To overcome this problem of autocorrelation a new variable (5 x DEPTH + DISTIN) was created utilizing the finding that DEPTH has 5 times the effect on PROD as DISTIN per foot of change. A stepwise multiple linear regression analysis with PROD as the dependent variable and (5 x DEPTH + DISTIN), DISTL, LINDEN, INTDEN, and LENTH as the independent variables revealed that the model:

$$\log_e(PROD) = 5.08 - 0.00132\ (5 \times DEPTH + DISTIN) \quad (8)$$

explained 81% of the variability in well productivity and was significant at the 0.0001 level. As Figure 7 shows, the model predicts the productivities of the 29 wells examined with a reasonable degree of accuracy.

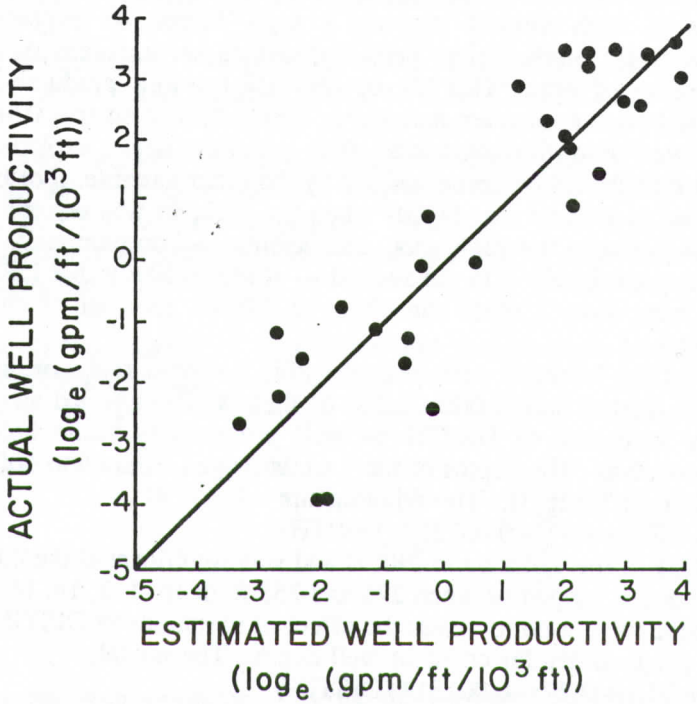

Figure 7. Comparison between actual well productivity and the productivity predicted by model (8).

The simplicity of the model means that it can be used to predict well productivity before drilling commences if fracture traces in the vicinity of the possible well site are mapped. Figure 8 provides a simple means of estimating productivity and also shows how well productivity varies with changes in DEPTH and DISTIN. The diagram illustrates that the productivities of wells of the same depth decrease away from a fracture trace intersection and that at any location well productivity decreases with increasing well depth. For example, for a 100 ft deep well productivity drops from 83.1 - 5.9 gpm/ft/10^3 ft as DISTIN increases from 0 - 2,000 ft. At a fracture trace intersection productivity declines from 83.1 - 3.1 gpm/ft/10^3 ft as well depth is increased from 100 - 600 ft, and at a distance of 2,000 ft from a fracture trace intersection productivity drops from 5.9 - 0.2 gpm/ft/10^3 ft over the same range of well depth.

CONCLUSIONS

The study of 257 wells in the crystalline Piedmont and Blue Ridge Mountain regions of Georgia has shown that there is no significant relationship between well productivity and lithology — a finding that is in agreement with research

conducted by Davis and Turk (1964). However, the data did reveal that well productivity decreased significantly as well depth increased — a trend that has been reported previously by other workers (Mundorff, 1948; Davis and Turk, 1964; Summers, 1972; Welby and Wilson, 1982).

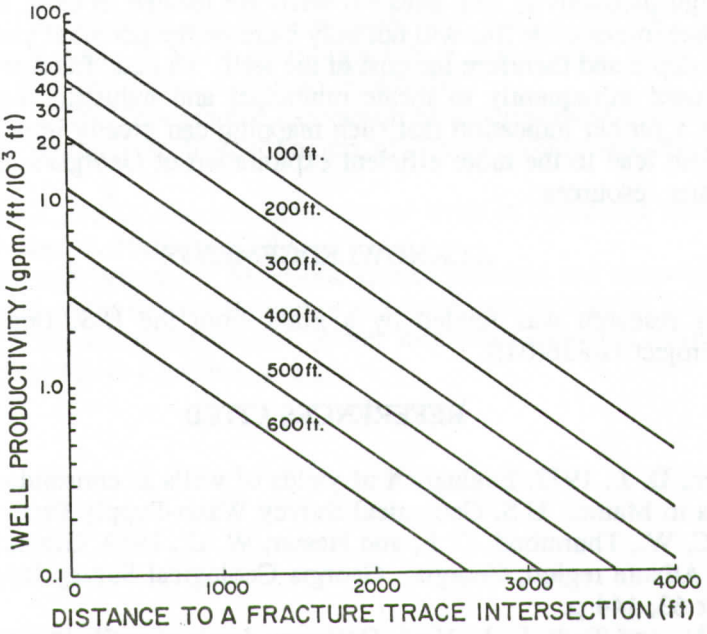

Figure 8. Relationships between well productivity, well depth, and distance to a fracture trace intersection according to model (8).

The detailed study of 29 wells revealed that relationships between well productivity and well depth, such as that obtained here using data for 257 wells, can be misleading. The finding that well depth depends to a large degree on well location — in particular on distance to a fracture trace intersection — indicates that some of the explanation of productivity ascribed to depth by such relationships should really be accounted for by well location factors. Studies of wells with the same depth, and studies of wells at the same distance from a fracture trace intersection, showed that DEPTH affects well productivity 5 times more than DISTIN per foot of change. However, as the range of DISTIN values is approximately 5 times the range of well depths, these two variables seem to have approximately the same effect on well productivity in the Georgia crystalline terranes. The simple model:

$$\log_e(\text{PROD}) = 5.08 - 0.00132\ (5 \times \text{DEPTH} + \text{DISTIN}) \qquad (8)$$

explained 81% of the variability in well productivity. This model suggests that as wells are drilled deeper they tap a diminishing water supply as water-holding fractures become less numerous, less-well integrated, and more tightly closed. It also indicates that there is a similar reduction in water availability away from a fracture trace intersection — presumably because open, water-filled fractures are concentrated near bedrock fracture zones and they become less numerous at increasing distance from these zones.

The simplicity of the model developed means that it can be used (through diagrams like Figure 8) by well drillers and water resources planners to locate high-productivity wells in the crystalline rock regions of Georgia. The model suggests that fracture trace mapping on aerial photographs can provide information useful in locating high-productivity well sites. If wells are located as close as possible to a fracture trace intersection this will not only increase the potential yield but will also reduce the depth and therefore the cost of the well. To date, fracture trace mapping has been used infrequently to locate municipal and industrial well sites. This research is a further indication that such mapping can greatly improve well yields and therefore lead to the more efficient exploitation of Georgia's crystalline rock, ground-water resources.

ACKNOWLEDGEMENTS

This research was funded by a grant from the U.S. Department of the Interior (Project G-836(04)).

REFERENCES CITED

Cederstrom, D. J., 1972, Evaluation of yields of wells in consolidated rocks, Virginia to Maine: U.S. Geological Survey Water-Supply Paper 2021, 38 p.

Cressler, C. W., Thurmond, C. J., and Hester, W. G., 1983, Ground water in the greater Atlanta region, Georgia: Georgia Geological Survey Information Circular 63, 144 p.

Davis, S. N., and Turk, L. J., 1964, Optimum depth of wells in crystalline rocks: Ground Water, v. 22, p. 6-11.

Harman, D. H., Watson, D. A., and Duffey, T., 1984, Georgia's Piedmont ground water: Water Well Journal, v. 38(2), p. 33-38.

Heath, R. C., 1979, Better utilization of ground water in the Piedmont and Mountain region of the southeast. *In*: Water Conservation and Alternative Water Supplies (eds. J. R. Wallace and B. Kahn), Environmental Resources Center, Georgia Institute of Technology, Atlanta, p. 145-160.

Lattman, L. H., 1958, Technique of mapping geologic fracture traces and lineaments on aerial photographs: Photogrammetric Engineering, v. 24, p. 568-576.

Lattman, L. H., and Nickelson, R. P., 1958, Photogeologic fracture trace mapping in the Appalachian plateaus: American Association of Petroleum Geologists Bulletin, v. 42(9), p. 2238-2245.

Ledbetter, J. L. and Herwig, R. A., 1979, Current and near-term water supply/demand problems in Georgia. *In*: Water Conservation and Alternative Water Supplies (eds. J. R. Wallace and B. Kahn), Environmental Resources Center, Georgia Institute of Technology, Atlanta, p. 23-29.

LeGrand, H. E., 1967. Ground water of the Piedmont and Blue Ridge provinces of the southeastern states: Circular 538, United States Geologic Survey, 11 p.

LeGrand, H. E. and Mundorff, M. J., 1952. Geology and ground water in the Charlotte area, North Carolina: Bulletin 63, North Carolina Department of Conservation and Development, Division of Mineral Resources, Raleigh, North Carolina, 88p.

Mundorff, M. J., 1948. Geology and ground water in the Greensboro area, North Carolina: Bulletin 55, North Carolina Department of Conservation and Development, Division of Mineral Resources, Raleigh, North Carolina, 108 p.

Parizek, R. R., 1976, On the nature and significance of fracture traces and lineaments in carbonate and other terranes. *In*: Karst Hydrology and Water Resources, Volume I: Karst Hydrology (ed. V. Yevjevich), Water Resources Publications, Fort Collins, Colorado, p. 47-100.

Staheli, A. C., 1976, Topographic expression of superimposed drainage on the Georgia Piedmont: Geological Society of America Bulletin v. 87, p. 450-452.

Summers, W. K., 1972, Specific capacities of wells in crystalline rocks: Ground Water, v. 10(6), p. 37-47.

Welby, C. W. and Wilson, T. M., 1982, Use of geologic and water yield data from ground water based community water systems as a guide for ground water planning and management: Water Resources Research Institute, University of North Carolina, 111 p.

LATE PLEISTOCENE CLIMATIC FACTORS IN THE GENESIS OF A CAROLINA BAY

DANIEL J. BLILEY — *Department of Soil Science, NC State University, Raleigh, NC 27607*

DAVID A. BURNEY — *Dept. of Biological Anthropology & Anatomy, Duke University, Durham, NC 27710*

ABSTRACT

Soils and sediments of a Carolina bay located on the Piedmont-Coastal Plain contact zone were investigated. Wilson's Bay (Johnston Co., NC) exhibits some unusual features, including gravelly rim sediments, probably resulting from ice-push activity, and saprolite that outcrops within the bay and at the bay's edge. Other bay surficial sediments consist of a prominent well-sorted sandy unit on the NE rim and a distinct silty unit in the depression. These surficial units unconformably overlie a buried soil surface with high organic content and adjacent truncated soils formed in saprolite and Coastal Plain sediments. The buried soil surface represents a former poorly-drained upland depression. The existing oval-shaped bay formed by expansion of this depression during an open-water phase, as shown by the lateral sediment relationships within the surficial deposits. Pollen studies indicate that vegetation characteristic of the late Pleistocene existed at the site during the deposition of the buried soil profile and surficial sediments. The onset of the bay's open-water phase (radiocarbon dated to a minimum of 22,000 yr B.P.) was accompanied by a shift to colder and possibly wetter climatic conditions.

The gravelly rim sediment units are similar to ice-push deposits that have been described along the shores of modern lakes in the northern U.S. and southern Canada. Further evidence of ice-push activity comes from the sorted nature of the deposits, the apparent formation of the deposits concurrent with a shift to colder climate, the relationship of the deposits to an adjacent saprolite surface which has been depleted of coarse fragments, and the large size of some of the transported stones.

The distinct sandy rim unit is believed to be partly eolian in origin, deposited by strong southwesterly winds. The distribution of the basal sands in the fine-textured surficial deposit reflects the influence of the SW wind on shoreline erosion, sediment transport, and the orientation of the bay. Initial bay expansion, however, did not correlate with the SW wind component.

INTRODUCTION

Carolina bays are shallow elliptical depressions that are formed on undissected land surfaces on the Atlantic Coastal Plain. Most of the bays are bordered by sandy rim deposits and commonly exhibit other unusual features, such as bays within bays and multiple intersecting bays. Because of these unusual features the bays have been given considerable attention in the literature over the

last 50 years. Descriptions of the features as well as various hypotheses of origin are well-documented (e.g., Johnson, 1942; Prouty, 1952; Kaczorowski, 1977).

Several studies within the past twenty years (Thom, 1970; Kaczorowski, 1977; Bliley and Pettry, 1979; Gamble and others, 1975) have presented evidence that the bays are primarily surficial features and are most likely formed from less distinct upland depressions. These became flooded and underwent expansion and orientation by erosion of shorelines under the influence of climatic conditions associated with the late Pleistocene. Under this hypothesis, strong directional winds in conjunction with cooler and wetter climates are believed to be the dominant factor in bay genesis. Pollen studies and radiocarbon dates (Whitehead, 1981; Frey, 1955) have confirmed the late Pleistocene age of these bays and provided some general evidence as to climatic conditions.

Although this hypothesis has been given general acceptance, few studies have actually involved detailed mapping and characterization of bay sediments to provide evidence that would adequately explain many of the unusual features of Carolina bays. One reason is that bay soils and sediments are not always distinctly different from adjoining interbay soils, and it is often difficult to distinguish features related to bay genesis from those of adjoining Coastal Plain sediments.

The bays are significant because their soils are widespread and many apparently have a unique genesis (Daniels and others, 1984). That they are apparently climatic relics is also significant because further studies could provide more detailed evidence about late Pleistocene climates in the southeastern United States, a region where detailed paleoclimatic evidence is generally sparse.

GEOLOGIC SETTING

This study focuses on Wilson's Bay, a Carolina bay located in Johnston County, NC, near the community of Wilson's Mills. This area (Figure 1) is a transition zone where Middle Coastal Plain sediments and saprolites from metamorphic rocks outcrop in complex patterns (Bliley and others, in press). Part of this complexity is due to the undulating nature of the saprolite surface and the erosional nature of much of the overall landscape. There is a distinct gravel layer which consistently occurs at the contact between the Coastal Plain sediments and the underlying saprolite.

The Brandywine Coastal Plain terrace in the vicinity of Wilson's Bay is not of great areal extent. At least two terrace levels are present which are moderately dissected by ephemeral and perennial streams. This bay is formed on one of the few undissected interstream areas. This unit (Terrace II, Figure 1) has a surface elevation ranging from 70-73 m. At the NW and SE ends of the bay are remnants of a higher-lying terrace unit (Terrace I, Figure 1), with surface elevations ranging from 76-79 m. Escarpments occur where the bay is formed against these higher upland units. The most prominent of these is at the SE end of the bay, where there is ca. 5 m of relief.

Wilson's Bay has the distinct oval form and rim sediments which are characteristic of most bays; however, preliminary studies revealed several features not described in studies of other bays: 1) there are gravelly sedimentary units associated with the sandy rim sediments; 2) a distinct silty sediment unit occupies the bay depression, which is underlain by a buried soil surface; and 3) the bay was

partly formed in saprolite, which outcrops along the prominent escarpment at the SE end of the bay.

Because of the distinct nature of the bay sediments and the unusual setting, it was decided that detailed mapping of bay sediments and studies of the underlying buried organic materials might provide more specific evidence as to the mechanisms of bay genesis and associated climatic conditions.

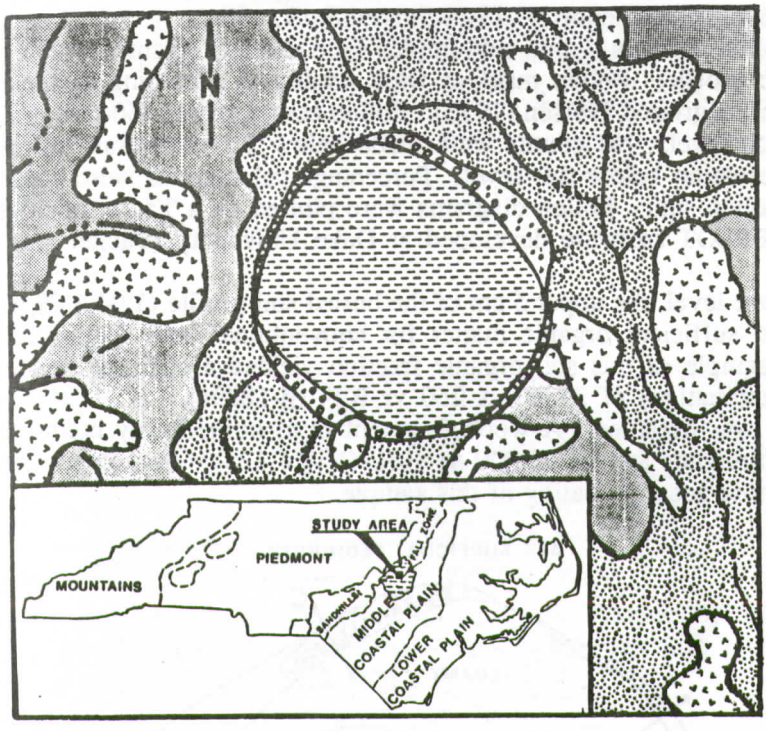

Figure 1. Location and surficial geology of the study area.

METHODS

Bay sediments and contacts with underlying materials were mapped by hand auger transects and random borings. Surface elevations along the transects were determined by transit and stadia rod. Soil and sediment colors and textures were

described utilizing standard USDA terminology (USDA, 1951). Specific locations of bay morphologic features were plotted from aerial photography at scales of 1:15,840 and 1:4800. A detailed description of the bay stratigraphy was made from a pit excavated along the NE-SW transect (Figure 2, Transect A). Samples from morphologic horizons were collected for particle-size, chemical, and mineralogical analyses. Soil samples were analysed according to methods outlined in Soil Survey Investigations Report #1 (Soil Survey Staff, 1984).

For pollen analysis, 1 cm^3 subsamples were taken at 20 cm intervals from the stratigraphic profile. Pollen residues were processed according to the methods described in Faegri and Iversen (1975). Pollen counts of ca. 450-600 grains were made at each level. No counts were made below 2.1 m because of very poor pollen preservation below this level. Percentage calculations were based on the terrestrial pollen sum. Pollen diagrams were plotted on a Tandy microcomputer using COREPLOT software developed at Duke University (Tucker and Tucker, 1985).

Only one level, the upper 5 cm of the buried soil profile (1.04-1.09 m, Figure 3) contained sufficient organic matter for conventional beta decay radiocarbon dating. A sample of this soil organic fraction yielded a ^{14}C age (corrected for isotopic fractionation) of 21,920 ± 260 yr B.P. (β-18296). A $^{13}C/^{12}C$ ratio of -31.28 0/00 was obtained. A wood fragment from immediately below this layer yielded a minimum age of 25,000 yr B.P. (NWV-123). Equipment limitations prevented more accurate dating of this sample.

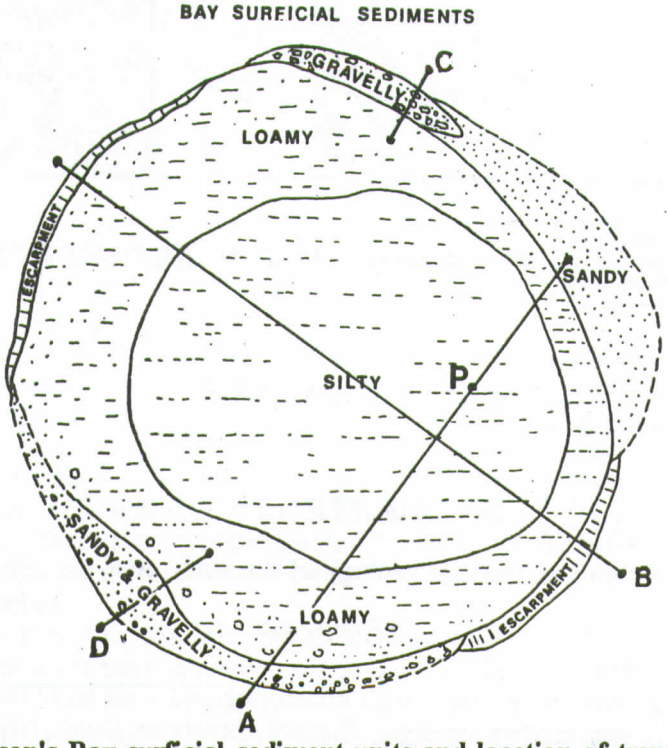

Figure 2. Wilson's Bay surficial sediment units and location of transects. Symbol (P) is location of detailed stratigraphic description site.

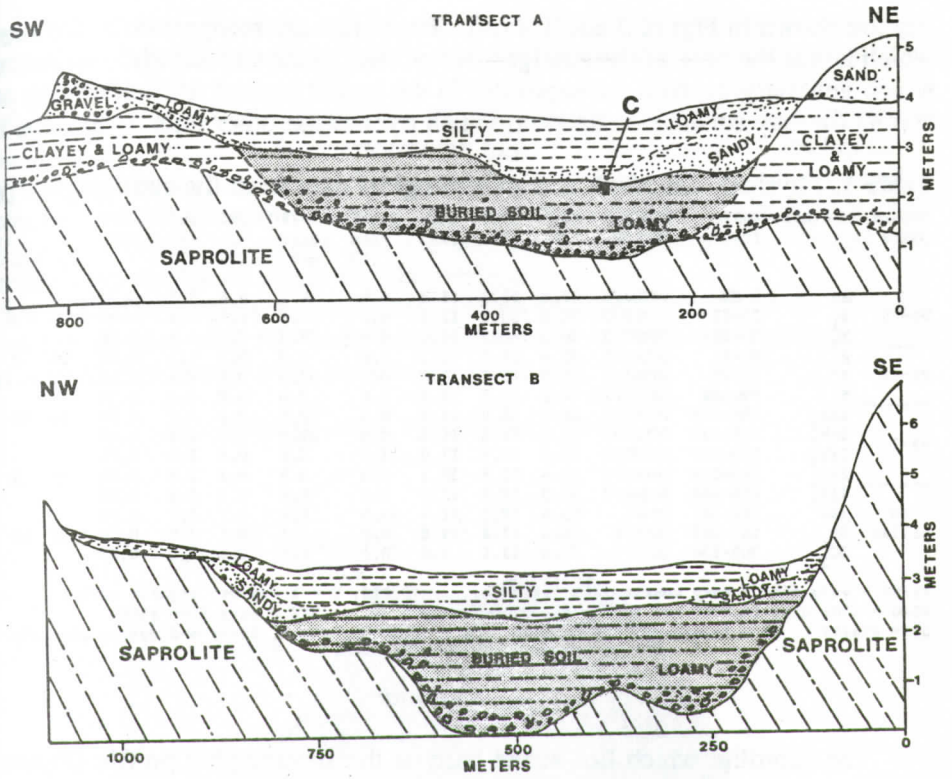

Figure 3. Geologic cross section along the short axis (Transect A) and the long axis (Transect B) of Wilson's Bay. Note the vertical exaggeration. Symbol (C) indicates location of level ^{14}C dated to 21,920 ± 260 yr B.P.

BAY MORPHOLOGY

The central portion of the bay depression is flat, which is typical for Carolina bays. This is a distinctive feature in this locality because adjacent uplands are somewhat convex. The edges of the bay are sharply defined in the NE and SE-SW sectors (Figure 2). The other edges of the depression are somewhat less well defined. Orientation of the long axis of the depression is approximately 305°. The NE rim unit is topographically distinct, with 1-2 m of relief (Figure 3). The S and SW rims are rather indistinct when observed from within the bay. However, they are somewhat more discernible when viewed from the bay exterior. Rim sediments are lacking in the NW and SE quadrants, where escarpments are formed against adjacent uplands. The most prominent escarpment is along the SE edge. Overall the natural drainage within the depression is poor, as it is in the interbay areas to the SW and NE of the bay. The adjoining Terrace I interbay uplands to the NW and SE are well-drained.

GENERAL STRATIGRAPHY

The relationship between the major stratigraphic units within and beneath the

bay are shown in Figure 3 and Table 1. Four units are recognized: 1) the saprolite, which lies at the base of the stratigraphic profile; 2) the Coastal Plain sediment unit, which generally overlies the saprolite; 3) the buried surface and underlying profile; and 4) the bay surficial sediments, which overlie the other units within the bay.

Table 1. Physical, chemical, and mineralogical data from the stratigraphic profile.

POLLEN ZONES	HORIZON	DEPTH (CM)	MUNSELL COLOR	SAND (%)	SILT (%)	CLAY (%)	COARSE >2mm (%)	VF/VC SAND RAT.	ORG. C (%)	pH 1:1 H_2O	FC/C RAT.	VFS (%)	MINERALOGY (%)		
												QZ	FD	MI	OR
	Ap	0-25	10YR2/2	18.8	55.7	25.5	0.0	6.8	5.4	5.5	0.30				
WB-2b	B_1	25-53	10YR5/3	24.6	53.2	22.2	0.0	39.5	1.1	4.8	0.48	95	3	1	1
——	B_2	53-81	10YR5/3	36.5	48.3	15.2	0.0	79.3	0.8	4.5	0.50				
	E	81-91	10YR7/2	70.4	26.3	3.3	1.0	7.8	0.2	4.5	0.69	96	2	<1	1
WB-2a	B'	91-99	10YR5/1	17.3	65.7	17.0	0.0	33.6	0.5	4.4	0.48				
——	E'	99-104	10YR7/1	74.2	22.5	3.3	1.0	7.4	0.2	4.4	0.90				
	$2Ab_1$	104-119	10YR2/1	44.2	38.9	16.9	0.5	10.5	3.6	4.1	0.50	98	<1	<1	1
WB-1	$2Ab_2$	119-150	10YR2/1	32.9	42.5	24.6	0.2	22.2	1.7	3.8	0.48				
	$2Ab_3$	150-193	10YR3/3	55.1	29.9	15.0	1.3	3.4	0.1	3.9	0.56				
——	$2Ab_4$	193-226	10YR2/2	32.4	33.9	33.7	1.2	3.9	0.2	3.8	0.62	97	1	<1	>1
	$2Ab_5$	226-249	10YR4/2	68.3	19.2	12.5	6.9	1.9	0.1	3.9	0.68				
no	3Bb	249-287	5Y4/1	43.4	15.2	41.4	19.9	6.4	0.2	3.7	0.83				
pollen	$3C_1$	287-305	5GY6/1	66.4	13.8	19.8	0.0	5.5	0.1	3.9	0.50	28	60	12	<1
	$3C_2$	305-434	5GY6/1	77.6	13.4	9.0	0.1	4.6	0.0	3.9	0.38				

VF/VC = very fine / very coarse sand ratio ORG. C = % dry wt. organic carbon
FC/C = fine clay (<.0002 mm) / clay (<.002 mm ratio VFS = very fine sand
QZ = quartz FD = feldspar MI = mica OR = other resistant, heavy and opaque minerals

Saprolite

The saprolite which lies at the base of the stratigraphic profile (Figure 3) is formed from felsic gneiss (Farrar, 1985). This material generally has a uniform loamy texture, relict rock structure, and common macroscopic mica flakes which are typical of saprolites throughout the area. The high feldspar content of the layer at 2.87 m (Table 1) confirms the presence of saprolite at this depth.

The saprolite underlies the Coastal Plain sediment unit throughout most of the area. However, because of the undulating to sharply dipping nature of its surface (Figure 3) saprolite outcrops in areas on the level to gently-sloping uplands of Terrace I and II (Figure 1), and on erosional hillslopes and escarpments. It also directly underlies the bay surficial sediments.

The gravelly layer at the contact between the saprolite and the Coastal Plain sediments (Table 1: 2Ab5 and 3Bb) consists mainly of well-rounded to angular vein quartz with a few cobbles and small stones intermixed. Where the saprolite lies beneath the bay surficial sediments (Figure 4), the gravel content is low or the gravel is completely absent from the upper part of the saprolite-derived soil.

Coastal Plain Sediments

These sediments are somewhat more clayey than is typical for Middle Coastal Plain sediments throughout the general area (Bliley and others, in press). However, the presence of other clayey soil areas on Terrace II indicates that they may be common in this locality. These sediments may be Pliocene in age (Daniels and others, 1978), and they have been considerably altered through the processes of weathering and soil formation. Therefore few clues exist as to the nature of the original depositional environment. The clayey textures, however, suggest a low-

energy environment. The firm, sticky, and plastic consistency of many of the clay layers suggest the presence of a smectite component which is possible evidence of marine origin.

A well-developed soil profile is formed in the upper 1-1.5 m of these sediments on the upland areas exterior to the bay. The surface layers are typically loamy and less than 15 cm in thickness overlying a clayey or fine-loamy argillic horizon. Where this Coastal Plain sediment unit lies beneath the bay sediments, the loamy surface layers are absent and the bay surficial sediments lie directly on remnants of the clayey or loamy argillic horizon.

There are few gravels in these Coastal Plain sediments, except in the gravelly layer at the contact with the underlying saprolite. As with the saprolite, fossil pollen is generally absent from the Coastal Plain unit.

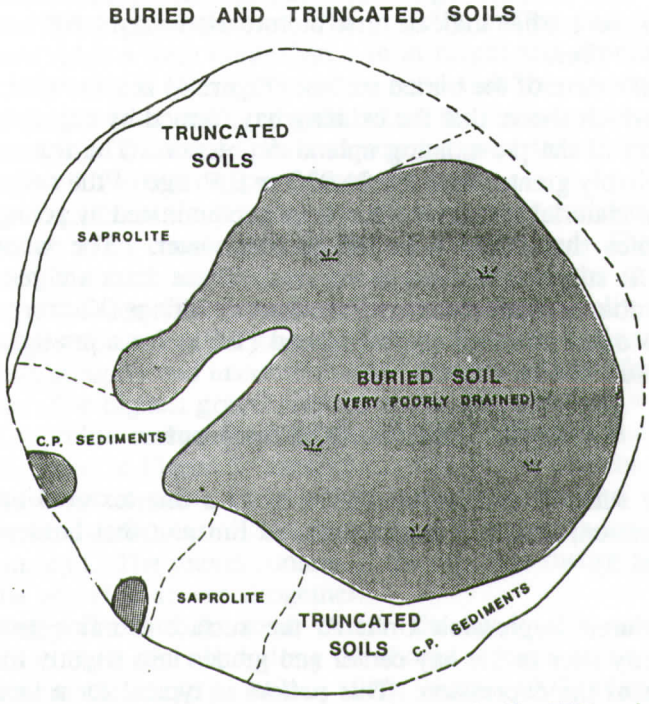

Figure 4. Buried and truncated surfaces which underlie Wilson's Bay surficial sediments.

Buried Surface and Underlying Profile

In the central and eastern portion of the bay (Figure 3), this unit occupies a similar stratigraphic position to the Coastal Plain sediment unit in other parts of the area. However, it differs from the Coastal Plain unit in that is has conspicuous dark colors throughout (Table 1). Other than organic accumulation, there is little physical evidence of the development of soil genetic horizons. At the profile description site, the percent fine clay of the clay maxima at 1.19 and 1.93 m is low (Table 1), which is evidence that these layers are more of a depositional rather than pedogenic nature. The accumulation of pollen grains that are relatively well-

preserved in the layers at 2.1 m and above, and the overall variability of the vf/vc sand ratio in these layers are further evidence for the cumulative nature of this profile.

Figure 3 shows that the buried surface previously occupied a topographic low, indicating that it was a shallow upland depression prior to burial. The low chroma and high organic content of the upper layers attest to the previously poor drainage conditions. All the evidence suggests that the buried soil occupies the surface of a pre-existing shallow depositional basin. The highly siliceous nature of the sand fraction of the layers at 1.04 and 1.93 m is evidence that the Coastal Plain sediments, which are typically siliceous, were a major source of the sediments in this basin. The stratified nature of the underlying profiles as well as the relatively indistinct horizonation suggest a relatively slow, possibly intermittent accumulation of sediments with variable depositional energy. The presence of some irregular boundaries in the profile indicate that bioturbation may have been significant at least part of the time.

The areal extent of the buried surface (Figure 4) is somewhat smaller than the present bay, which shows that the existing bay formed by expansion of the poorly drained portion of the pre-existing upland depression. The true age of the buried surface is probably greater than the 21,920 yr B.P. age of the soil organic fraction. It is likely that material at this level has been contaminated by younger carbon in the soluble organics that move with the ground water. The wood sample dated >25,000 yr B.P. suggests that this is the case. These dates are generally within the range of a number of other dates for Carolina bay fillings (Kaczorowski, 1977), and are similar to dates obtained by Whitehead (1981) for a stratigraphically similar layer from a bay in Chowan Co., NC.

Bay Surficial Sediments

The bay surficial sediments consist of 1) a fine-textured unit that occupies the bay depression, and 2) a coarse textured rim unit that borders the depression (Figures 2 and 3).

Fine-textured Depression Unit: At the surface the fine-textured depression unit is distinctly silty in the bay center and grades into slightly loamier sediments near the edge of the depression. This pattern is typical for a lacustrine sediment unit (Hutchinson, 1957). The base of this unit is coarser and, with the exception of some thin strata (Table 1), it consistently fines upward throughout the bay. Basal sediments also coarsen laterally and become distinctly sandy near the edge of the depression (Figure 3). This sediment sequence resembles a transgressive shoreline sequence on a small scale. An exception to this trend is the lens of sandy material that extends into the bay center from the sandy unit along the NE shoreline. At this point the basal sandy material is thicker than at other sectors along the bay's edge. This thicker sandy unit also lies adjacent to the prominent sandy rim sediment unit.

It is not likely that much of the sediment of the fine-textured depression unit was derived by surface erosion from adjoining upland areas, because the bay has little or no exterior watershed and there are no streams or drainageways that empty into the bay. The lateral sequence of sediments within the surficial depression unit

suggest that it was mainly derived by erosion of shoreline into sediments and saprolites that bordered a smaller pre-existing depression. Further evidence for this is that, in the truncated soil zone (Figure 4), the surficial sediments lie abruptly and unconformably on remnants of B horizons that are formed either in the Coastal Plain sediments or in saprolite. This is made evident by the characteristic fining-upward sequence of the surficial unit, which contrasts with the underlying, primarily clayey, subsoils. The low but significant feldspar content of the upper layers of the surficial sediment (Table 1) is additional evidence that the adjoining saprolite-derived soils were in part the source of this sediment.

Rim Sediments: The rim sediments are characteristically coarse-textured throughout. The NE rim of this bay is topographically more distinct than the SW rim unit. One reason for this is that the adjoining Coastal Plain units are slightly higher along the NE edge of the bay. The gravelly unit on this rim consists of a relatively narrow ridge a little more than 1 m in height and about 18 m in width. Where this gravel merges laterally with the sand unit the rim becomes broader (Figure 2), and the rim is ca. 60 m in width where the distinct sandy unit is located. Most of the sand from the sandy rim unit was removed for construction material during the 1950's (C.W. Wilson, pers. comm.).

The coarse fraction of the gravelly unit is mainly well-rounded to angular vein quartz gravels with a few cobbles and small stones intermixed. The size and shape distribution of this coarse material is identical to that of the gravel layer that consistently caps the saprolite throughout the area. The gravelly rim unit differs from the saprolite cap in that the matrix consists of clean, well- sorted sand, and the rim unit rests abruptly and unconformably on truncated soils formed in Coastal Plain sediments. The highest gravel content of this unit coincides with the adjacent outcrop of the saprolite surface beneath the surficial sediments immediately within the bay, as illustrated in Figure 5, transect C. The gravel content of this rim unit diminishes where the saprolite surface dips beneath the Coastal Plain sediments adjacent to the sandy rim unit. There are only a few gravels associated with the broad sandy rim unit. The gravel content of the saprolite surface within the bay is very low or the gravel is absent altogether.

The gravelly rim and, to some extent, the sandy rim, resemble ice-push deposits that have been described along the shores of lakes in the northern United States and southern Canada (e.g., Miller, 1970; Dionne, 1972; Wagner, 1970). Ice-push deposits are formed when the edge of an ice mass is thrust against low-relief shorelines, forcing sediments into ridges. The sediment normally consists of coarse material previously sorted by other shoreline processes. Ice push is caused by the expansion of the lake ice due to temperature and phase changes. Also, following the break-up of an ice mass, wind may drive shoreward ice blocks bearing sediment.

The climates in the regions where modern ice push occurs are generally cold temperate, with extremely cold winter temperatures and wide temperature fluctuations. There is also a pronounced spring thaw followed by a break-up of lake ice. A similar cold temperate climate may have existed at this locality at the initiation of the open-water and expansion phase of the bay.

The most obvious source of the gravel in the gravelly rim unit is the gravel that capped the adjacent saprolite surface within the bay. Ice push is the most likely

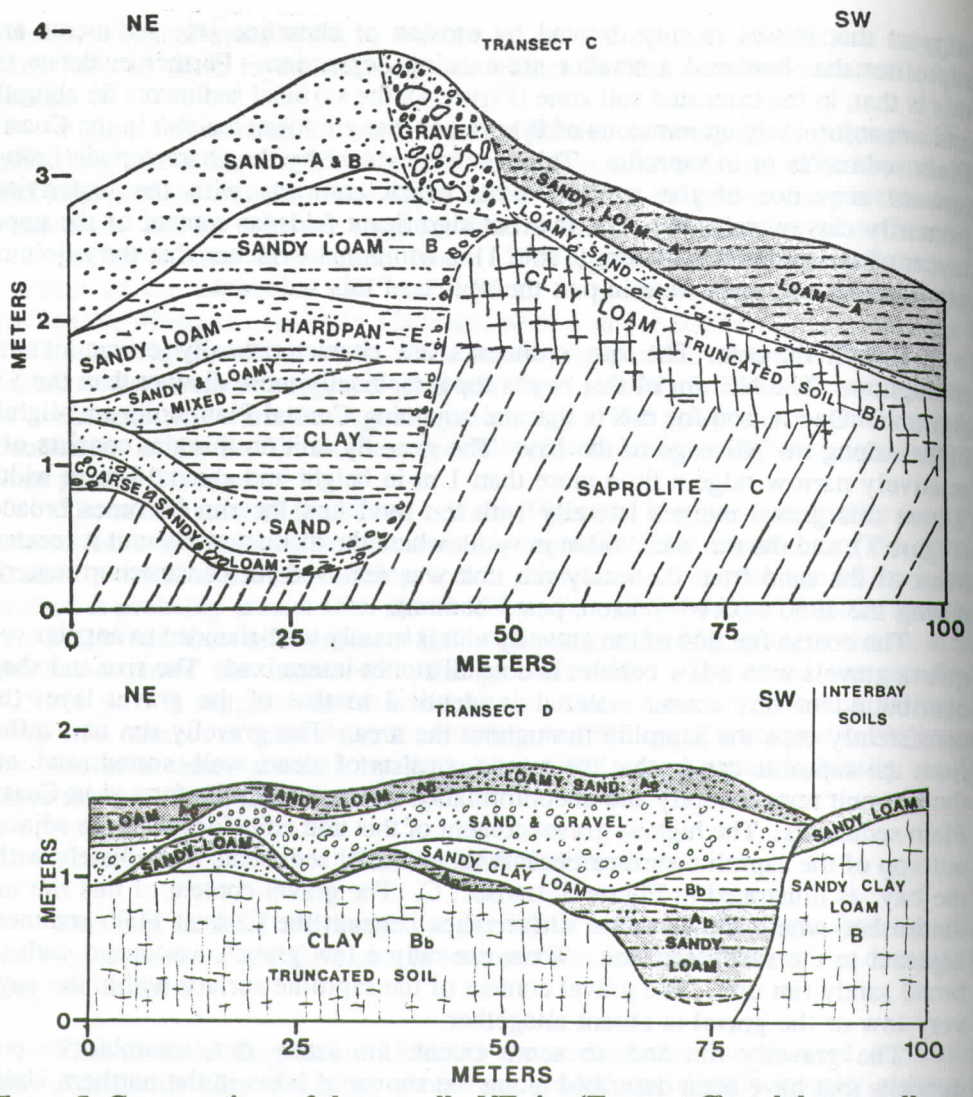

Figure 5. Cross sections of the gravelly NE rim (Transect C) and the gravelly and sandy SW rim (Transect D) of Wilson's Bay.

mechanism for the transport and deposition of this material. The sorted nature of this deposit, the unconformable contact with the underlying sediments, and the climatic conditions that are inferred from the pollen data to follow provide evidence that this mechanism was involved. Also, the energy requirements for transport of this coarse material (stones to 40 cm in diameter) are too great to be accounted for by conceivable alternative mechanisms.

Along the S and SW edges of the bay the rim sediment units are barely discernible when viewed from within the bay (Figure 5, Transect D). The reason for this is that the interior surface of the bay, which is nearly obscured by the fine-textured surficial unit (Figure 3) is slightly higher than the exterior surface. Also there are no thick sandy deposits along this rim such as on the NE rim. The gravel

content is more variable than along the NE rim, which may be due to the less extensive outcrop of saprolite along the rim and within the bay adjacent to this rim. These rim sediments gradually merge with the basal sand lens that underlies the fine-textured surficial depression unit. The rim sediments in this case actually appear to be coarser and thicker terminal members of the basal sandy sub-unit.

There are two areas (Figure 4) where the SW rim sediments overlie isolated small areas of buried surfaces that are poorly drained. These areas also lie in the vicinity of the modern topographic drainageways immediately exterior to the bay (Figure 1). Some of the buried sediments, such as the pocket of sandy loam Ab material beneath the edge of the rim (Figure 5), resemble alluvial sediments found in some modern drainageways. The poor drainage of these buried surface remnants and their association with the modern topographic drainageways indicate that they were probably part of the drainage outlet for the former upland depression. The fact that the rim sediments overlie these surfaces is additional evidence that the formation of the rims was instrumental in blocking the drainage outlet and maintaining a high water level in the bay.

Although most of the sand has been removed from the prominent sandy unit on the NE rim, it was possible to determine the areal extent from 1937 aerial photographs of the bay. That this unit was a distinct topographic feature was confirmed by the landowner (C.W. Wilson, pers. comm.) and other local inhabitants. Furthermore, remnants of a rim unit almost identical in form and relative location still exist on another bay located about 1 km to the north of Wilson's Bay.

There is a distinct bulge (Figure 2) in the rim at the location of this sandy deposit, which has the form of a parabolic dune. Similar units were recognized by Gamble and others (1975) in other bays and were believed to be caused by "eolian or aqueous activity, or both." The well-sorted nature of this sandy deposit as well as the parabolic form are evidence that eolian processes were involved. However, the association of this unit with the adjacent gravelly rim also suggests that other processes (e.g. ice thrusting) were involved in its formation.

Prevailing SW winds were probably involved in the deposition of the eolian component of this rim unit. The smooth, sharply-defined edges of the bay depression in the NE and SE quadrants are additional evidence that these shorelines were reworked by waves generated by SW winds. Longshore currents generated by this wind component would have been maximized along the N and E shorelines. These shores would have been zones of maximum erosion and sediment transport. The lee shore adjacent to the sandy rim would be a zone of sediment accumulation because of the converging currents. At this point a subsurface return current should be generated in a direction opposite to that of the prevailing wind (Kaczorowski, 1977). The relatively thick accumulation of sand along this lee shore and the extension of the sand toward the bay center (southwestward) are evidence that this type of erosion and transport mechanism was operational during bay formation. The probable effect of ice push on the formation of the eolian unit would be to position the sand onto the shoreline for redistribution.

POLLEN STUDIES

Figure 6 shows percentages for the major pollen types identified in the

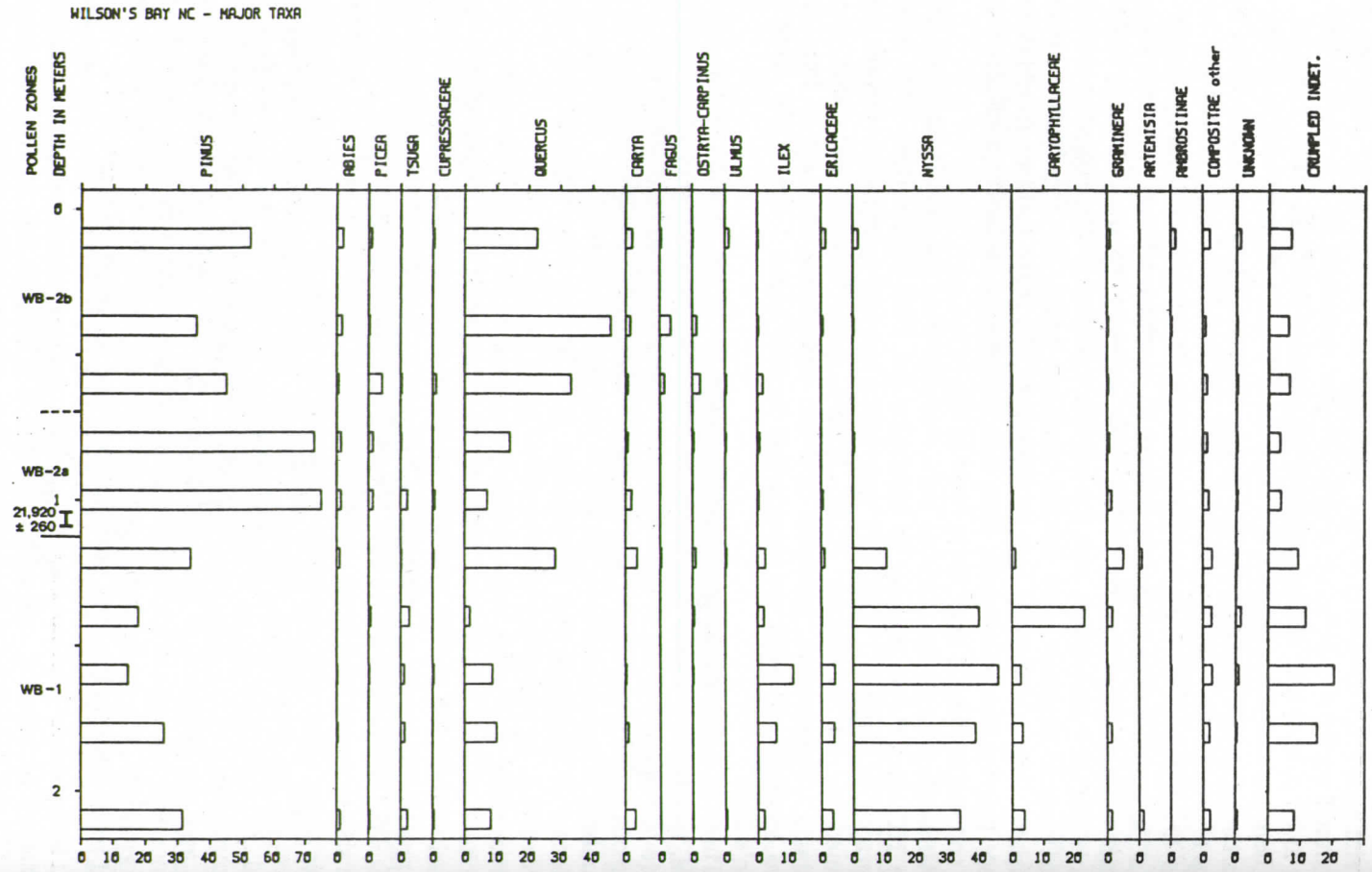

Figure 6. Percentage diagram for major pollen types identified from Wilson's Bay stratigraphic description site.

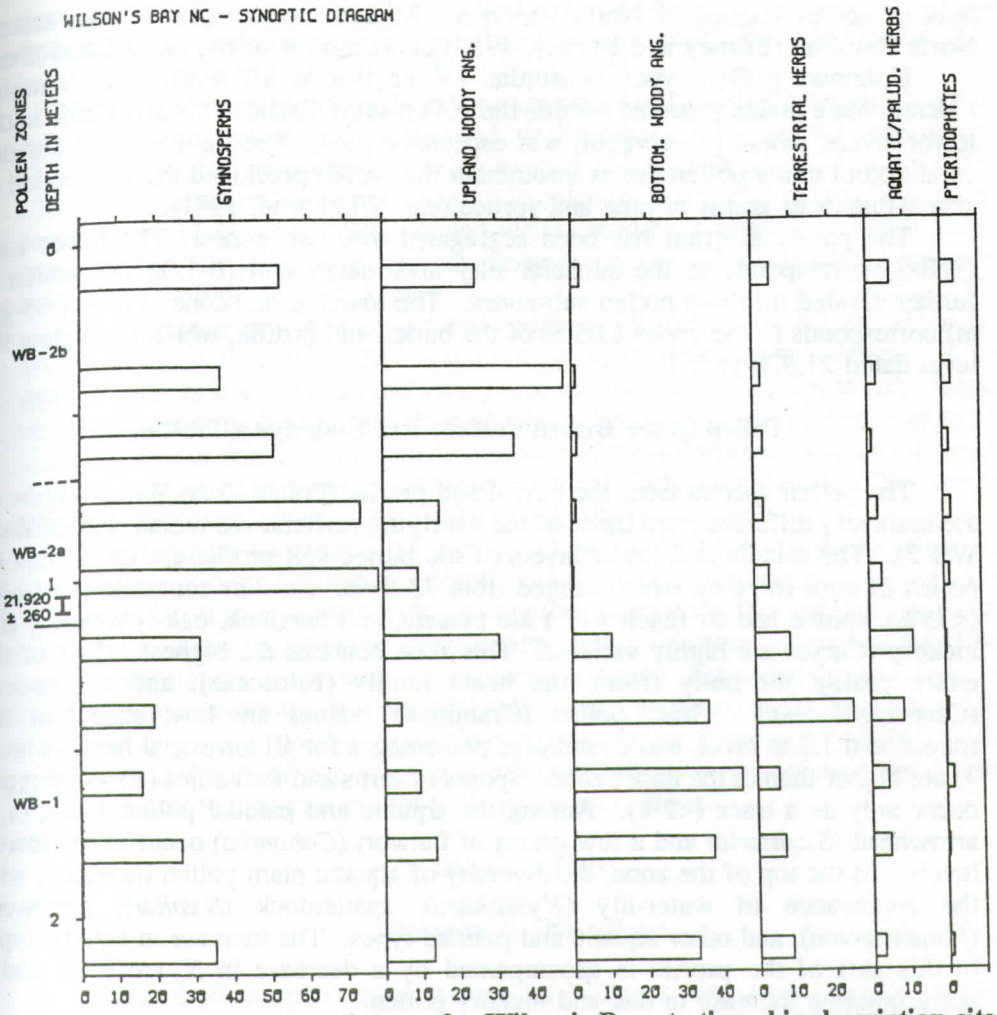

Figure 7. Synoptic pollen diagram for Wilson's Bay stratigraphic description site. Ecological groupings generally follow Burney and Burney (1987). Key to abbreviations: ang. = angiosperms; bottom. = bottomland; palud. = paludal.

stratigraphic profile and Figure 7 provides a synopsis of the pollen data. The presence of numerous pollen types associated with boreal forest and other environments which are presently restricted to more northerly latitudes or higher elevations confirms the Pleistocene age of the surficial sediments and buried profile. Many of the pine pollen grains identifiable to the species level were of jack pine (*Pinus banksiana*) and red pine (*P. resinosa*). A few white pine (*P. strobus*) grains were identified at some levels. Other major taxa probably indicative of Pleistocene age include fir (*Abies*), spruce (*Picea*), and hemlock (*Tsuga*). Among minor taxa (not shown on diagram) were such Pleistocene indicators as tamarack (*Larix*), jointweed (*Polygonella*), curly-grass fern (*Schizaea pusilla*), soapberry (*Shepherdia canadensis*), and stiff club-moss (*Lycopodium annotinum*). These types of pollen and spores come from plants presently found

only in colder regions of North America. Modern pollen spectra from eastern North Carolina (Burney and Burney, 1987) contain none of the types listed above.

Unknown pollen types constitute 1% or less at all levels, but crumpled indeterminate grains (counted outside the pollen sum) reached as high as 20% in the lower levels, where preservation was especially poor. The flattened and abraded condition of many pollen grains throughout the profile precluded the application of size statistics to grains of pine and spruce (e.g. Whitehead, 1981).

The pollen diagram has been segregated into two zones. The upper zone (WB-2) corresponds to the surficial silty and loamy unit (0-1.05 m), which is further divided into two pollen sub-zones. The lower zone (Zone WB-1, 1.05-2.1 m) corresponds to the upper 1.05 m of the buried soil profile, which lies below the level dated 21,920 yr B.P.

Pollen in the Buried Surface and Underlying Profile

The pollen spectra from the buried soil profile (Pollen Zone WB-1, Figure 6) are markedly different from those of the overlying surficial sediments (Pollen Zone WB-2). The middle and lower layers of the buried soil profile are dominated by pollen of gum (*Nyssa*), which ranged from 33-44%. Smaller components of pine (<35%), spruce and fir (each <1%) are present, and hemlock, oak (*Quercus*), and hickory (*Carya*) are highly variable. This zone contains the highest values of the entire profile for holly (*Ilex*), the heath family (Ericaceae), and chickweeds (Caryophyllaceae). Grass pollen (Gramineae) values are low, except at the transitional 1.2 m level, and cumulative percentages for all terrestrial herbs (Figure 7) are higher than in the upper zone. Spores of ferns and fern allies (Pteridophytes) occur only as a trace (<2%). Among the aquatic and paludal pollen types, only arrowhead (*Sagittaria*) and a few grains of fanwort (*Cabomba*) occur in the lowest levels. At the top of the zone, the diversity of aquatic plant pollen increases, with the appearance of water-lily (*Nymphaea*), spatterdock (*Nuphar*), pondweed (*Potamogeton*), and other aquatic and paludal types. The increase in aquatic types in this part of the profile is accompanied by a decrease in *Nyssa* (9%) and a corresponding increase in oak and hickory pollen.

The pollen spectra from the middle and lower parts of the buried soil profile indicate that deposition was probably in a swampy woodland with little or no standing water. Evidence for this is the presence of gum and other woody bottomland plants that probably grew on the sediment surface. These plants are associated with present-day bottomlands in the Atlantic Coastal Plain. Both boreal and temperate plants shared the surrounding uplands during deposition of the buried soil profile. These data suggest that climatic conditions were somewhat cooler or less seasonal than today.

Pollen in Surficial Sediments

The pollen spectra of the various layers in the surficial sediment unit differ from those of the underlying buried profile. In this unit there is a general decline of gum, holly, and heaths to <2% at all levels (Figure 6). The lower part of this unit (WB-2A, 0.7-1.1 m) has the highest values for pine (>70%) of the entire stratigraphic profile and very low values for all terrestrial herbs. The pine pollen of

these spectra are dominated by the red pine and jack pine (*P. resinosa, P. banksiana*) assemblage characteristic of other southeastern sites during the Full Glacial of the late Wisconsin (e.g. Watts, 1980, Whitehead, 1981).

Most warm-temperate pollen types are completely absent from this subzone. Paludal pollen types, notably arrowhead, decline sharply, but aquatic types persist. This suggests that an open-water body existed at least part of the time. The Full Glacial vegetation reflects a marked shift to colder climates, which accompanied the development of the pond. The ponded water could be indicative of higher annual precipitation, but lowered evapotranspiration, perhaps coupled with a moderate increase in rainfall, is more likely.

In the upper part of the surficial sediment (WB-2B, 0.6- 0.1 m), there is a decline in pine values to 40-50% and a corresponding increase in temperate upland species such as oak, which reaches a maximum of 48% at 0.4 m. Beech (*Fagus*) becomes important for the first time, reaching 3.3% at 0.4 m. Highest values are also recorded in this sub-zone for hornbeams (*Ostrya-Carpinus*) and elm (*Ulmus*). A rise in these types is highly characteristic of Early Postglacial pollen spectra from the Southeast (Watts, 1980; Whitehead, 1981).

The topmost spectrum (0.1 m), which is in the plow zone, contained no recognizable pollen of introduced plants, although corn (*Zea mays*) is cultivated on the site today. It also showed <1% grass pollen, despite the fact that grassland is an important component of the modern environment. The poor representation of the modern vegetation in the topmost spectrum suggests that sediment accumulation and pollen preservation at this site probably slowed or ceased at the beginning of the Holocene or before. Pollen types characteristic of the Pleistocene occur near the surface as a result of the high soil moisture and acid conditions, which have preserved late Pleistocene microfossils in the soil matrix.

DISCUSSION

Relation to Other Bays

The overall morphological features of Wilson's Bay, such as the oval form and orientation, are generally similar to those of bays described from other areas in the southeastern Coastal Plain. The lack of well-defined margins in the W and NW sectors of the depression is typical of many other bays as well. The geologic setting is unusual in that no reports describe Carolina bays that are formed in saprolite. However, Carolina bays have in fact been described from a wide variety of other geologic settings. Thom (1970) suggested that bay formation could occur in practically any type of undissected land surface that originally may have contained less distinct depressional areas. Although Kaczorowski (1977) reported that buried soils and sediment layers commonly occurred within bay depressions, other studies (Bryant and McCracken, 1964; Gamble and others, 1975) suggest that distinct buried soil surfaces (such as in Wilson's Bay) are not common in bay depressions.

Wilson's Bay has many features common to Carolina bays in general. One distinctive feature lacking, however, is the well-developed sandy rim that is formed at the SE end of many bays further south and east in North and South Carolina. Apparently sandy rims were not formed at the SE end of bays in this specific

locality. Further evidence for this is the absence of a sandy SE rim on a nearby bay north of Wilson's Bay. Perhaps this is evidence for the variability of factors involved in rim deposition throughout the region. It is possible that more intensive studies of this particular phenomenon could shed additional light on this aspect of paleoclimates.

Bay Genesis

The presence of a buried soil surface beneath the bay surficial sediments is evidence that a poorly-drained depression existed at this location prior to the formation of the bay. This depression apparently did not have a well-developed drainage outlet. The stratified nature of the underlying profile and the presence of abundant fossil pollen is evidence that the original depression was also a shallow depositional basin with intermittent periods of deposition in a swampy woodland environment.

There are few clues as to the origin of the initial depression, because the Coastal Plain sediments have probably undergone considerable weathering and physical alteration since their deposition. Closed upland depressions, however, are not common, but they do occur on a few relatively undissected Coastal Plain land surfaces within the region.

The pollen data suggest that there may have been a gradual transition from the upland swamp to the relatively permanent open water stage of the depression. The permanent water stage was probably accompanied by a shift to colder climate. There is no clear evidence of a significant increase in precipitation, although the colder temperatures would likely result in lowered evapotranspiration. This would contribute to the development of open water at the site. The low relief as well as the presence of the clayey layer which caps the underlying saprolite (Table 1, 3Bb) would also serve to maintain poor drainage. The possible development of ice-push ridges may have raised the level of the drainage outlet, thus providing a mechanism for maintaining the high water level in the depression. Figures 2,3, and 5 show that the postulated ice-push sediment along the SW rim probably acted in this capacity during the latter stages of sedimentation. It is likely that this mechanism was effective in the earlier stages of bay development as well.

The existing bay is considerably larger than the original depression, which is approximated by the area of the buried surface (Figure 4). Expansion and orientation of this depression occurred mainly by erosion of the shorelines into adjacent soils formed in Coastal Plain sediments and saprolites. The textural relationships within the fine-textured depression unit as well as the presence of truncated soils underlying this sediment are evidence that the depression was enlarged by this process. The presence of eolian sands along the NE edge as well as the presence of ice-push rim sediments would indicate that wind-driven waves and currents as well as ice thrusting influenced shoreline erosion processes and bay expansion.

Ice Push

The primary evidence that the coarse-textured (gravelly) rim sediments are ice-push deposits is that their deposition coincides with the development of the

open water and expansion phases of the bay during the onset of cold conditions. The pollen and radiocarbon evidence indicate that this ice activity most likely coincided with the onset of the last glacial maximum of late Wisconsin times. The local climatic conditions during this time, as inferred from the jack pine/red pine-dominated pollen spectra, were perhaps comparable to those that are presently found in the upper Great Lakes, the northeastern U.S., and southern Canada, where these trees are found today. It is in these cold temperate regions that modern ice-push sediments have been described along the shores of lakes as cited earlier.

Ice-push deposits are formed when the edge of the lake ice is thrust against the shoreline, forcing sediment into narrow ridges. Wagner (1970) reported that the formation of ice-push sediments is often complicated by local conditions. However, when all other conditions are favorable, the presence of a low shoreline with shallow incline will favor ice push. Thermal expansion of the ice mass and the thrusting ashore of ice blocks by strong winds following break-up of the ice are considered to be the primary mechanisms for ice push. Pessl (1971) suggests that thermal expansion is the primary mechanism for ice push on small lakes. Hobbs (1911) asserts that thermal expansion is most influential on small lakes 0.5 to 1.5 miles in diameter. Wilson's Bay fits into this small-lake category for thermal expansion. It is likely, however, that wind-thrusting of ice blocks was also involved in the formation of the NE ice push rim because of its association with the adjoining eolian sand unit.

Ice push is a relatively high-energy mechanism. It has been observed to uproot trees, move large rocks, and destroy man-made structures along lake shorelines (Ruhe, 1975). The deposition of relatively large (40 cm diameter) fragments in the NE gravelly rim of Wilson's Bay is further evidence for ice activity, as no substitute mechanism has been found in this context which could generate sufficient energy to move such heavy objects.

Basin Expansion and Orientation

Kaczorowski (1977) proposed that basin expansion was a stage that preceded bay orientation. He suggested that strong directional winds perpendicular to the bay's long axis influenced orientation, but he did not specify whether directional winds or another separate mechanism was involved in the initial expansion. The presence of the eolian body along the NE edge of the bay, as well as a corresponding adjacent sand accumulation within the bay in this sector, is evidence that a SW wind component with accompanying waves and currents was effective in orienting the bay by eroding and smoothing the contour of shorelines along the SE and NE edges of the bay.

Apparently factors other than strong prevailing paleowinds were involved in bay expansion. Figure 4 shows that most of the expansion occurred in southerly and westerly directions. There do not appear to be any other eolian units that would have influenced erosion along this shoreline. Ice push as well as the freeze-thaw action associated with cold temperatures would have been effective agents in destabilizing shorelines and making them more susceptible to erosion by wave action generated by winds from other directions.

The role of paleowinds in shaping and orienting Carolina bays is still not entirely clear, although longshore currents generated by strong prevailing winds

were almost certainly an important factor. However, evidence presented in this paper for the role of ice push in the formation of Wilson's Bay suggests that the significantly colder temperatures inferred for the Wisconsin glaciations, perhaps coupled with wide fluctuations in winter temperature, may have played a key role in bay genesis. Most studies of Pleistocene conditions in the Southeast have concluded that mean annual temperatures were lower in the region, without clarifying whether the vegetation differences were primarily a reflection of cooler summers or colder winters, or both. The existence of ice-push features confirms that winters were considerably colder than at present.

CONCLUSIONS

1. Wilson's Bay was formed from a smaller, pre-existing shallow depression.
2. This small basin was expanded by the erosion of shorelines during an open-water phase. The initiation of this phase has a minimum radiocarbon age of ca. 22,000 yr B.P.
3. The expansion phase occurred in response to a shift toward colder climatic conditions.
4. The gravelly rim sediments that were deposited concurrent with basin expansion are ice-push ridges.

ACKNOWLEDGEMENTS

Funding for the radiocarbon dates and much of the soil laboratory characterization data was provided by the National Soil Survey Laboratory of the Soil Conservation Service, U.S. Dept. of Agriculture, in Lincoln, Nebraska. We thank Warren Lynn for assistance in coordinating this laboratory work. Additional laboratory data were provided by the Dept. of Soil Science, N.C. State University. Stanley Buol and Russ Robertus assisted with this portion of the study. Pollen analysis was conducted in the Zoology Dept. at Duke University using facilities supported by NSF grants to D.A. Livingstone and D.A. Burney. Livingstone provided useful comments on an early draft of the manuscript, and R.B. Daniels and E.E. Gamble assisted with conceptualization of the study.

REFERENCES CITED

Bliley, D.J., and Pettry, D.E., 1979, Carolina Bays on the Eastern Shore of Virginia: Soil Sci. Soc. Am. Jour. 43, 558-564.

Bliley, D.J., and others, in press, Soil survey of Johnston County, NC. USDA Soil Conservation Service, Washington.

Bryant, J.P., and McCraken, R.J., 1964, Properties of soils and sediments of Carolina Bays: J. Elisha Mitchell Sci. Soc. 80, 166.

Burney, D.A., and Burney, L.P., 1987, Recent paleoecology of Nags Head Woods on the North Carolina Outer Banks: Bull. Torr. Bot. Club 114(2), 156-168.

Daniels, R.B., Gamble, E.E., and Wheeler, W.H., 1978, Age of soil landscapes in the coastal plain of North Carolina: Soil Sci. Soc. Am. Jour. 42, 98-105.

Daniels, R.B., Kleiss H. J., Buol, S. W., Byrd, H. J., and Phillips, J. A., 1984, Soil Systems in North Carolina: N.C. Agricultural Research Service Bull. 467, N.C. State Univ., Raleigh.

Dionne, J.C., and Laverdiere, C., 1972, Ice-formed beach features from Lake St. Jean, Quebec: Can. J. Earth Sci. 9, 979-990.

Faegri, K., and Iversen, J., 1975, Textbook of Pollen Analysis: Munksgaard, Copenhagen, 295 p.

Farrar, S.S., 1985, Stratigraphy of the northeastern North Carolina Piedmont: Southeastern Geology 25, 159-183.

Frey, D.G., 1955, A time revision of the Pleistocene pollen chronology of southeastern North Carolina: Ecology 36, 762-763.

Gamble, E.E., Daniels, R.B., and Wheeler, W.H., 1977, Primary and secondary rims of Carolina Bays: Southeastern Geol. 18, 199-212.

Hobbs, W.H., 1911, Requisite conditions for the formation of ice ramparts: J. Geol. 19, 157-160.

Hutchinson, G.E., 1957, A Treatise on Limnology, 1. Geography, Physics, and Chemistry: Wiley, New York, 1015 p.

Johnson, D.W., 1942, The Origin of the Carolina Bays: Columbia U. Press, New York, 342 p.

Kaczorowski, R.T., 1977, The Carolina Bays: A Comparison with Modern Oriented Lakes: Tech. Rept. No. 13-CRD, Coastal Research Director, Dept. of Geology, Univ. of South Carolina, Columbia.

Miller, G.A., 1970, A geomorphic, hydrologic, and pedologic study of the Iowa Great Lakes area: M.S. thesis, Iowa State Univ., Ames, Iowa, 333 p.

Pessl, F., Jr., 1971, Formation of a modern ice-push ridge by thermal expansion of lake ice in southeastern Connecticut: U.S. Cold Regions Res. Eng. Lab., Res. Rep. 259, 13 pp.

Prouty, W.F., 1952, Carolina bays and their origin: Geol. Soc. Am. Bull. 63, 167-224.

Ruhe, R.V., 1975, Geomorphology: Houghton-Mifflin, New York.

Soil Survey Staff, 1984, Soil survey laboratory methods and procedures for collecting soil samples: Soil Survey Investigations, Rep. No. 1, USDA Soil Conservation Service, Washington.

Thom, B.G., 1970, Carolina bays in Horry and Marion Counties, South Carolina: Geol. Soc. Am. Bull. 81, 783-814.

Tucker, V.A., and Tucker, A.E., 1985, A microcomputer data management program for plotting pollen diagrams: Pollen et Spores XXVII(2), 277-288.

United States Dept. of Agriculture, 1951, Soil Survey Manual: USDA Handbook 18, 503 pp.

Wagner, W.P., 1970, Ice movement and shoreline modification, Lake Champlain, Vermont: Geol. Soc. Am. Bull. 81, 117-126.

Watts, W.A., 1980, Late Quaternary vegetation history of White Pond on the inner coastal plain of South Carolina: Quaternary Research 13, 187-199.

Whitehead, D.R., 1981, Late Pleistocene vegetational changes in northeastern North Carolina: Ecol. Monogr. 51, 451-471.

MAGNETIC SURVEY OF THE WESTERN SERPENTINITE BELT, NORTHERN HARFORD COUNTY, MARYLAND*

MIMI J. FREEMAN**
D. F. PALMER
R. A. HEIMLICH

Department of Geology, Kent State University, Kent, OH 44242

ABSTRACT

Geophysical modeling of a ground magnetic and previously published aeromagnetic survey was undertaken to test alternative hypotheses of the structural relationships between the Baltimore-State Line mafic complex and the ultramafic bodies of the western serpentine belt near Cardiff and Whiteford, Maryland. Petrographic studies and magnetic susceptibility determinations were used to form the basis of three-dimensional prismatic models of high susceptibility serpentinite within schists of the enclosing Wissahickon terrane. Results show the bodies to be podiform to lenticular and conformable to the trend of the enclosing schists. The positions of near surface boundaries of the magnetic bodies may be controlled in part by alteration and oxidation related to the thick saprolite in this section of the Piedmont. Some of the boundaries are consistent with faulted contacts related to the strike slip fault which cuts the north side of the Peach Bottom structure. The shapes of serpentinites agree with the interpretation of Southwick (1969) but are not consistent with the thrust fault model implied by Crowley (1976). The serpentinites are similar to many other such bodies which occur throughout the formations of the Wissahickon terrane and may represent the disjointed rubble incorporated into a mélange during ophiolite emplacement.

INTRODUCTION

The Baltimore-State Line Complex is one of the largest genetically-related assemblages of mafic and ultramafic rocks in the Appalachians. The origin of the complex has been controversial for at least two decades. Work by Hopson (1964) and Southwick (1969) led to models involving magmatic emplacement of a layered complex prior to or during extensive deformation of the area. On the other hand, Thayer (1967) argued that the complex is an alpine type ultramafic body. A succinct review of the arguments for alpine or ophiolitic versus magmatic stratiform origin for the mass is related by Southwick (1970). In consonance with plate tectonic theory, the complex has been described as an ophiolite by Crowley (1976), Morgan (1977), and Fisher and others (1979) who suggest that the main mass and smaller subsidiary bodies are sections of oceanic lithosphere emplaced on the continent in Taconic time. Drake and Morgan (1981) studied the Piney Branch Complex in Virginia and proposed that it and the Baltimore-State Line Complex

*Contribution No. 352, Department of Geology, Kent State University, Kent, Ohio 44242.

**Present address: Solar Testing Lab, 9540 Midwest Ave., Garfield Heights, Ohio 44125

were separate fragments of a single central Appalachian ophiolite. Their map of the region from Fairfax County, Virginia to Pennsylvania suggests that the tectono-stratigraphic horizon of the Piney Branch Complex is the same as that of the disconnected serpentinite bodies west of the Baltimore-State Line Complex. More recently, Shaw and Wasserburg (1984) conducted an investigation of Nd and Sr isotopic signatures in mafic-ultramafic complexes in the Appalachians and California. Their work showed isotopic differences between different ophiolites and demonstrated the presence of an old crustal isotopic component in the mafic rocks of the Baltimore-State Line Complex which appears to preclude an origin from strictly oceanic crust and depleted upper mantle.

Shaw and Wasserburg (1984) note further the probable diverse origins of the ultramafic rocks of the Appalachians based on isotopic data. This conclusion is certainly consistent with the earlier geologic and chemical work of many investigators who have documented evidence leading to conflicting ideas on the origin of the ultramafites in the region (see, for instance, Southwick, 1970; Chidester & Cady, 1972; Misra and Keller, 1978).

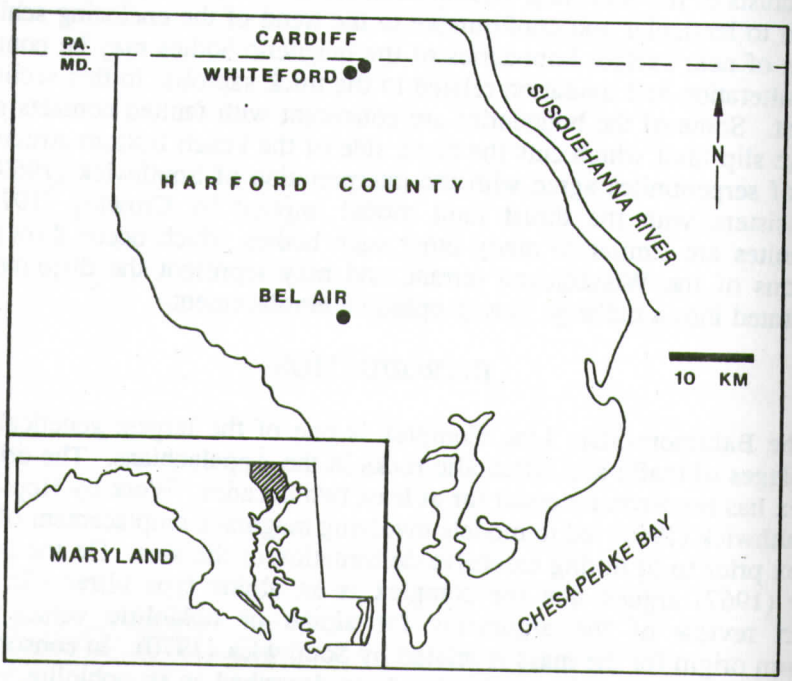

Figure 1. Location map of Harford County, Maryland.

In Harford County, Maryland (Figure 1), ultramafic rocks occur as a clear northern extension of the Baltimore-State Line Complex and as a series of thin, discontinuous serpentinite bodies trending N65E in a linear belt 33 km in length (Figure 2). These latter bodies constitute the Western Serpentinite belt in Harford County and have been interpreted as the western-most edge of the Baltimore-State Line Mafic Complex (Hopson, 1964) even though there is no clear connection with the major mafic rock terrane to the south and east. The main mafic complex is enclosed by metasedimentary rocks of the Wissahickon terrane (Drake and

Morgan, 1981) which is dominated by muscovite-quartz schists and metagraywacke and is disordered and stratigraphically chaotic (Crowley, 1976; Morgan, 1977).

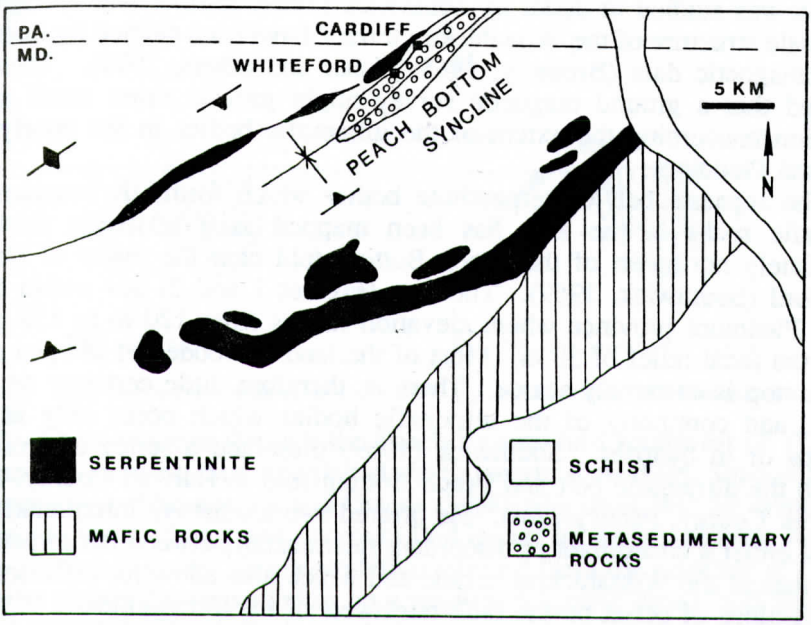

Figure 2. Generalized geologic map of northern Harford County, Maryland.

Recent studies of the central Appalachian Piedmont in Virginia and Maryland have shown the existence of a series of lithologically diverse mélange units whose origins may be both tectonic and sedimentary (Muller and Edwards, 1985; Muller and Others, 1985; Pavlides, 1985). Drake (1985a) suggests that the mélanges were formed as sedimentary slide deposits originating from large subaqueous thrust sheets which now overlie the mélanges. The slabs of ophiolite contained within certain of the mélanges may similarly have been resedimented blocks disrupted from larger ophiolite masses such as the Baltimore State Line complex. Drake and Morgan (1981) and Drake (1985b) note the occurrence of ophiolite blocks and slabs within a magnetic mélange unit termed the Peter's Creek Schist.

Younger (?) metasedimentary units, the Cardiff Metaconglomerate and Peach Bottom Slate, crop out along the axis of the Peach Bottom structure located immediately southeast of the Western Serpentinite Belt (Figure 2). The geometry and age relationships of the units in this fold are controversial. Early maps show the feature as a syncline, however, Higgins (1972) discussed the area in detail and concluded that the fold is an anticline. The schists in the area are complexly folded, but foliation strikes generally northeast and dips steeply, 70° to vertical, both to the north and south (Southwick, 1969).

Research on ultramafic bodies in Harford County began with mapping by E.B. Matthews at the turn of the century (Clark, 1898, 1907) and with petrographic studies which determined the presence of two original rock types, peridotite and pyroxenite (Johannsen, 1928). Investigation of microstructures within grains of olivine, serpentine, and chromite showed three stages of serpentinization with

intervening deformational events (Lapham, 1962; Lapham and McKague, 1964). Detailed work on the chromite and other mineral deposits was summarized by Pearre and Heyl (1960). The mineralogy, petrology, structure, and origin of the complex was studied in detail by Southwick (1969, 1970). The stratigraphy and large-scale structure of the Wissahickon terrane have been studied by interpretation of aeromagnetic data (Bromery, 1968; Fisher and others, 1979). These studies indicated that a ground magnetic survey might provide more detail and better resolution concerning the extent of the ultramafic bodies in the poorly exposed Maryland Piedmont.

The separate belt of serpentinite bodies which forms the western limit of ultramafic rocks in the area has been mapped as a relatively thick section immediately northwest of the Peach Bottom fold near the towns of Cardiff and Whiteford (Southwick, 1969). The area (Figures 1 and 2) lies within the gently rolling Piedmont province where elevation ranges from 120 m to 150 m, with a maximum local relief of 30 m. Most of the land is wooded or in open cornfields and outcrop is extremely scarce. There is, therefore, little certainty on the sizes, shapes, and continuity of the ultramafic bodies which occur only as sporadic outcrops or in quarries. Southwick (1969) presented a series of cross-sections through the ultramafic belt and Peach Bottom fold in Harford County, Maryland, and York County, Pennsylvania. He offered two alternative interpretations which suggest either a concordant or discordant relationship between the serpentinite and the schists of the Wissahickon terrane and which also allow for different amounts and directions of offset on the fault northwest of the ultramafites.

Of major interest in these two interpretations is the question of whether the serpentinites were emplaced by faulting or whether they may be folded around the Peach Bottom structure to join the main mass of the Baltimore-State Line Complex in southeastern Harford County.

Crowley (1976) noted the importance of these serpentinites as well, calling them "fundamental to any discussion of the mafic complex..." (p. 26) and suggested that these bodies were the western fragments of the ophiolite complex. His interpretation of their positions was quite different from that of Southwick (1969) in that his map (Crowley, 1976, plate 2) shows the eastern contact of these bodies as a west-dipping thrust which cuts the stratigraphy and folding in part of the Wissahickon terrane.

The differences in the interpretations are striking and have clear tectonic significance (Figure 3). The investigation reported here was undertaken for the purpose of delineating the map outlines and three dimensional subsurface configuration including the attitude, thickness, and depth below the surface of the several poorly exposed serpentinites in the western serpentinite belt. Field work consisted of a ground magnetic survey and sampling of the sparse outcrops of serpentinite and country rock. Petrographic modal analyses, magnetic susceptibility determinations, and natural remanent magnetization measurements of samples were made to help interpret the magnetic survey results. The ground magnetic data were compared with available aeromagnetic surveys.

GEOLOGIC SAMPLING

Two quarries and a former asbestos pit provided the only exposures of

serpentinite for sampling (Figure 4). Samples were taken for petrographic modal analyses and magnetic susceptibility measurements. In addition, several oriented samples of serpentinite were obtained for determination of the remanent magnetization.

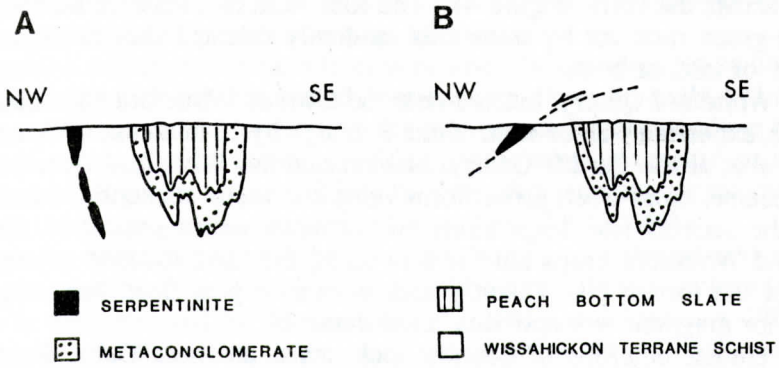

Figure 3. Cross sections through the Peach Bottom fold southwest of Whiteford (see Figure 2) showing two interpretations by previous workers. Section A gives the interpretation of Southwick and Owens (1968) who show that the serpentinites dip steeply to the southeast and are controlled in part by steeply-dipping strike-slip faulting. Section B shows an interpretation inferred from the mapping of Crowley (1976) who placed the serpentinites on a westward-dipping thrust fault which cuts the structures of the Peach Bottom syncline.

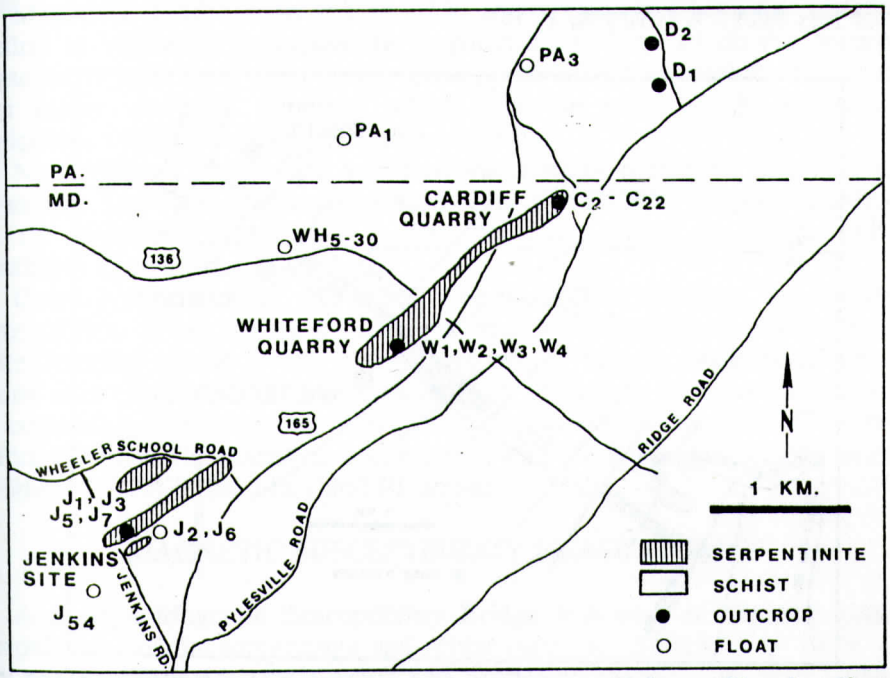

Figure 4. Previously mapped serpentinite outcrops and sampling locations for ultramafites and schists.

The Cardiff Quarry, a vertical pit measuring 18 by 40 m and 100 m deep, was operated by the Green Marble Company from 1890 until recently. Slabs of verde antique were quarried here for decorative and building stone; crushed material was marketed as granules for terrazzo floor covering (Pearre and Heyl, 1960). Serpentinite outcrops just north of the pit were sampled at 10 m intervals to study variation across the body (Figure 4). The rock here is a massive mottled light to dark gray-green rock cut by numerous randomly oriented thin to thick veins of magnesite, or talc, or both.

The Whiteford Quarry, located near the town of Whiteford and abandoned in the 1940's, exposes a wall of serpentinite 3 m high by 15 m across. The rock here is similar to that at the Cardiff Quarry; however, at the Whiteford Quarry, the rock displays coarse, cross-fiber, asbestiform veins and many slickensided surfaces.

At the Jenkins site, serpentinite with characteristics similar to the rock at Cardiff and Whiteford crops out for 6 m along the farm roadbed adjacent to the position of the former pit. Country rock occurs only as float, but samples were collected for magnetic susceptibility measurements.

The closest outcrops of country rock schist are near Delta, Pennsylvania (Figures 4 and 5) where several samples were taken. Additional schist samples were collected from float along traverses while conducting the ground magnetic survey.

PETROGRAPHY

Thin and polished sections were prepared from 14 serpentinite and four schist samples. Modal analyses were based on 1200 points per section, for an analytical error of less than 5% (Chayes, 1956).

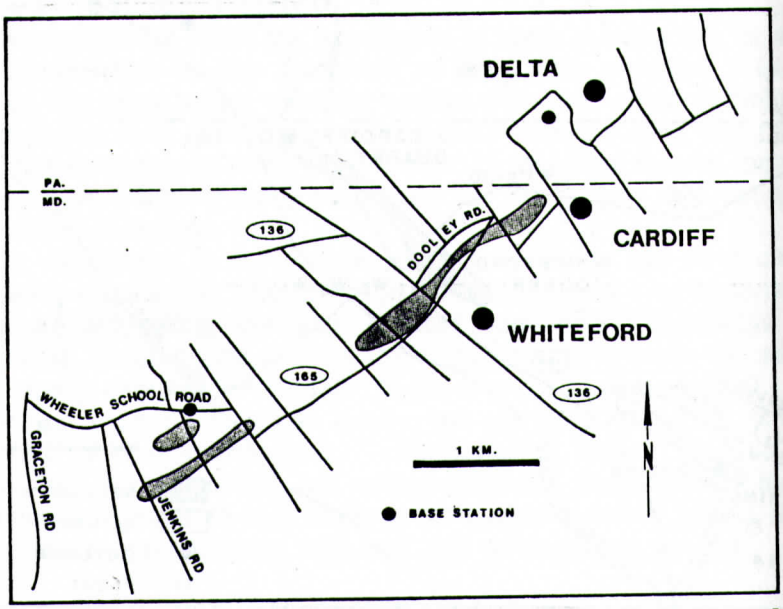

Figure 5. Location of base stations and magnetometer traverses along roads crossing the area.

All of the ultramafic rock samples are extensively altered (Table 1A). Although all primary olivine has been altered to secondary minerals, relict enstatite occurs in four samples ranging in amount from 0.1 to 10.7%. The serpentine occurs as slip-fiber and cross-fiber chrysotile veins which show a preferred orientation and display microfolds, microfaults, and twisting. They are cut locally by large patches of feathery antigorite which displays undulatory extinction. Bastite antigorite occurs pseudomorphous after enstatite.

Magnetite occurs in serpentinite as very fine-grained dust (not counted in the modal analyses) intimately associated with the serpentine minerals and as coarse coalesced masses of smaller grains and elongate grains distributed along chrysotile veins and bastite antigorite lamellae. Additionally, some magnetite is present as scattered euhedral grains and as primary skeletal fragments transected by feathery antigorite. Coarse magnetite ranges in volume from 0.8 to 4.4%.

Chromite, identified in polished section, occurs as euhedral and subhedral grains and ranges from 0.1 to 3.3% in seven of the serpentinite samples (Table 1A). Chromite is little affected by serpentinization (Condie and Madison, 1969; Saad, 1969), and most of the grains in the Maryland serpentinites are unaltered.

Talc content ranges from 0 to 65%. It occurs as patches and veins cutting the serpentine minerals and locally as large masses, the result of local CO_2-SiO_2 metasomatism as described by Williams and others (1982). Evidence of talc replacement of serpentine consists of linear aggregates of magnetite (some with limonite alteration) which occur in the masses of talc with small patches of serpentine remnants. Talc formed by alteration of serpentine is described from other ultramafic bodies in the Appalachians (Jahns, 1967; Misra and Keller, 1978).

Magnesite ranges from 0.1 to 36% and occurs in all of the samples as anhedral to subhedral rhombohedra in patches or veins which cut serpentine. Magnesite is associated with small cubic pyrite grains in most of the samples. Other minor alteration minerals, which occur in some of the samples, are vermiculite, chlorite, anthophyllite, and tremolite.

No significant mineralogic variation was detected across the body at Cardiff. One sample, however, is unusual because of its high (77.9%) tremolite content and lack of serpentine (Table 1A). The tremolite occurs as coarse radiating asbestiform aggregates.

Country rock samples, D1 and D2, obtained from outcrops, are muscovite-quartz schists. Float samples include a muscovite-quartz schist (PA-1) and a calcite-tremolite schist (J-2). Other samples of country rock float from the Jenkins area (Figure 4) were megascopically identified as tremolite-talc schist. The assemblage is thus similar to that detailed by Drake and Morgan (1981) around the Piney Branch Complex and is consistent with the lithologic findings of Fisher and others (1979) in the Maryland Piedmont.

MAGNETIC SUSCEPTIBILITY MEASUREMENTS

A Soiltest Magnetic Susceptibility Bridge was used to measure magnetic susceptibilities of the serpentinite and schist samples. As shown in Table 2, the mean susceptibilities for the Cardiff and Whiteford samples are almost identical (316 and 314 x 10^{-5} emu/cm^3) with a very large standard deviation in each case.

Table 1. Modal Analyses of Serpentinite and Country Rock Schist

A. Serpentinite

Sample#[1]	Serpentine	Talc	Magnesite	Enstatite	Tremolite	Vermiculite	Chlorite	Anthophyllite	Pyrite	Magnetite	Chromite	TOTALS
C2	79.2	16.9	0.4			0.3			0.1	1.2	1.8	99.9
C4	70.2		28.4			0.1				1.3		100.0
C6	93.0	0.1	3.5			0.1			0.1	3.0	0.1	99.9
C8	91.2	0.1	6.5	0.1		0.1				2.0		100.0
C10	92.7	0.7	4.4			0.1	0.1			1.0	1.0	100.0
C12	82.2	11.4	4.3				0.1			2.0		100.0
C16		17.6	1.9		77.9	0.2		0.1		2.1	0.1	99.9
C18	71.4	1.6	25.8	0.1		0.1	0.1		0.1	0.8		100.0
C20	89.6	0.1	2.0			0.1	0.1	0.3		4.4	3.3	99.9
C22	82.4	2.5	1.3	10.7	0.1	0.1	0.1		0.3	2.7		100.0
WI	32.0	65.0	0.1			0.9			0.1	1.8		99.9
W2	50.5	10.0	36.0			0.9				2.6		100.0
W3	39.0	39.4	17.2			0.5				2.7	1.1	99.9
JI	74.9	20.6	0.1	1.6						2.5	0.2	99.9

B. Country Rocks

Sample#	Muscovite	Quartz	Chlorite	Biotite	Calcite	Tremolite	Anthophyllite	Non-opaque Accessories	Magnetite	Chromite	TOTALS
J2			0.1		75.3	23.6	0.1		0.6	0.2	99.9
D1	44.3	38.9	12.5	3.5				0.5	0.3		100.0
D2	62.6	34.6	2.2	0.2				0.2	0.1		99.9
PA-1	89.8	6.5	2.3	1.2				0.1	0.1		100.0

[1] C = Cardiff; W = Whiteford; J = Jenkins; D = Delta; PA = Pennsylvania (for sample locations, see Figure 4).

Table 2. Magnetic Susceptibility Data for Serpentinite

Sample Number	Percent Serpentine	Percent modal Magnetite	Magnetic Susceptibility (10^{-5} emu/cm^3)
Cardiff Serpentinite			
C2	79.2	1.2	136.04
C4	70.2	1.3	154.37
C6	93.0	3.0	523.95
C8	91.2	2.0	267.93
C10	92.7	1.0	103.51
C12	82.2	2.0	265.57
C16	0.0	2.1	233.46
C18	71.4	0.8	147.51
C20	89.6	4.4	1082.80
C22	82.4	2.7	241.23
		Mean	315.63
		Standard Deviation	883.47
Whiteford Serpentinite			
W1	32.0	1.8	354.31
W2	50.5	2.6	289.96
W3	39.0	2.7	368.35
W4			244.45
		Mean	314.16
		Standard Deviation	99.96
Jenkins Serpentinite			
J1	74.9	2.5	220.26
J3			204.94
J5			197.99
J7			207.83
		Mean	207.75
		Standard Deviation	16.11
Mean for total serpentinite samples			291.35
Stand. deviation for all serpentinite samples			908.90

Samples from the Jenkins site have a lower mean susceptibility value and a much smaller standard deviation. Schist samples (Table 3) have a far lower mean susceptibility as compared with that for the serpentinites.

The overall mean for susceptibility values determined in this study falls between that for the Twin Sisters dunite in Washington (210 x 10^{-5} emu/cm^3) and that for a large number of serpentinite samples (600 x 10^{-5} emu/cm^3) from Red Mountain, California (Saad, 1969; Thompson and Robinson, 1975), but is much greater than means determined for partially serpentinized dunite samples (15.49 x 10^{-5} emu/cm^3) and for minimally serpentinized dunite samples (3.14 x 10^{-5} emu/cm^3) in North Carolina (Honeycutt and others, 1981; Schiering and others, 1982).

The measured susceptibilities for the serpentinite are markedly greater than those for the country rock schist, as expected from the modes where the magnetite

volume in the serpentinite averages 2.2% and only 0.2% for country rock.

Table 3. Magnetic Susceptibility Data for Schist

Sample Number	Magnetic Susceptibility (10^{-5} emu/cm^3)
J2	3.41
D1	93.91
D2	1.267
J6	1.18
J-54	57.43
PA-1	3.29
PA-3	1.32
WH5-30	76.80
Mean	29.82
Standard Deviation	104.50

NATURAL REMANENT MAGNETIZATION

Natural remanent magnetization (NRM) was found to be weakly positive in all samples analyzed. Thus, it was not considered to be an important effect in modeling of the magnetic data. NRM was also found to be weakly positive in similar ultramafic bodies in North Carolina (Honeycutt and others, 1981; Schiering and others, 1982; Hirt and others, 1987).

MAGNETIC SURVEY RESULTS

Field Procedures

The ground magnetic survey was conducted using a Geometrics proton precession magnetometer. Readings were made at a magnetic base station at approximately one-hour intervals during the day to correct for time-dependent drift in reducing of the data. Four readings were taken and averaged at each of over 2,000 stations. Stations were located on a network of 18 subparallel traverses with nine connecting or cross lines providing complete coverage over the area (Figure 5). Existing roads and paths were used but close to half of the traverses were located in woods and fields using pace and compass methods.

The resulting data were corrected for drift using standard techniques, and 52,000 gammas were subtracted from each point to arrive at the residual magnetic value at each station. The data were smoothed by a three-point running average and then were plotted and contoured, resulting in the ground magnetic map shown as Figure 6.

The magnetic contours parallel the NE-SW strike of the bodies, and the well-defined positive anomalies reflect the substantial magnetic susceptibility contrast between the serpentinite and the schist. Toward the serpentinite bodies, magnetic intensity increases gradually from 0 to 1200 gammas, then steeply to 2400 gammas at the northeast and to 2000 gammas to the southwest. The sharp peaks of these anomalies indicate the presence of serpentinite close to the surface. The wavelengths and the positions of the inflection points of the broader anomalies

indicate the presence of larger magnetic bodies at depth. Similarly, magnetic data for the Twin Sisters dunite exhibit the steepest gradient where slivers of serpentinite crop out, and a broad anomaly reveals the lateral extent of the serpentinite at deeper levels (Thompson and Robinson, 1975).

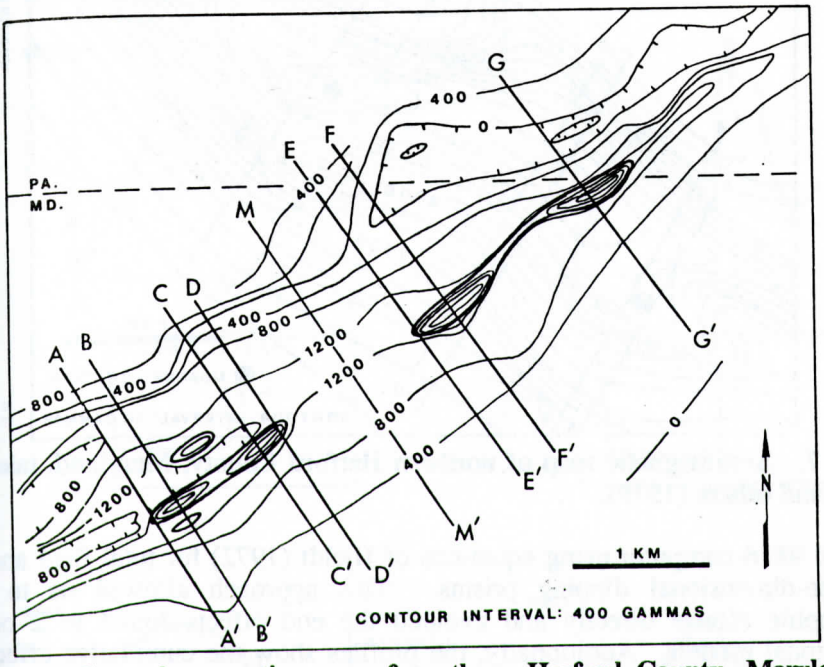

Figure 6. Ground magnetic map of northern Harford County, Maryland, and adjoining area in Pennsylvania with location of cross sections used in three-dimensional modeling.

Aeromagnetic Map

The total field aeromagnetic map (Figure 7) is reproduced from Bromery and others (1964) and shows the same linear trend of the data acquired at the surface. Magnetic intensity ranges from 7450 gammas to 8400 gammas, a difference of 950 gammas. The broader aeromagnetic anomaly with lower maximum gradients on its slopes reveals the lateral extent of the serpentinite in the subsurface and provides a second constraint on any geological model. Upward continuation of the ground magnetic data provides a close match to the aeromagnetic data. Although the serpentinite at the Whiteford and Jenkins sites is reflected by the more intense magnetic anomaly, the serpentinite outcrops at the Cardiff Quarry are not expressed in the aeromagnetic map, suggesting that the latter body is narrow and steeply dipping.

Modeling

The general outcrop patterns of other serpentinite bodies in Harford and Baltimore counties are consistent with the use of tabular and prismatic shapes to model the serpentinites within the area. Modeling was done with a Hewlett-

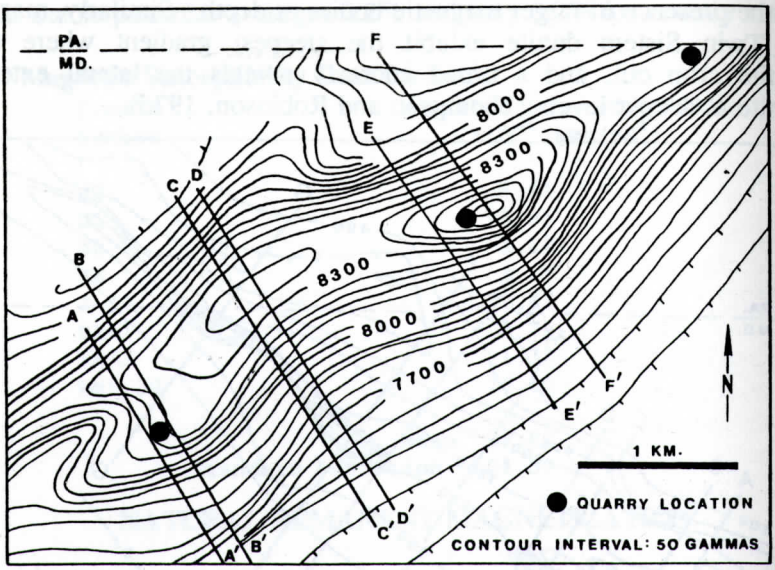

Figure 7. Aeromagnetic map of northern Harford County, Maryland, taken from Fisher and others (1979).

Packard 9816 computer using equations of Hjeldt (1972) for total field anomalies of three-dimensional dipping prisms. This approach allowed us to handle topographic effects directly and avoided the end effects found in 2 or 2 1/2 dimensional models. Additionally, the profiles show the cumulative effect of all bodies that occur away from the line of section in addition to those directly under the profile section.

The initial location and plan dimensions of the serpentinite bodies were determined by the location of the steepest magnetic gradients on the ground magnetic map. The steep dips of the schists of the enclosing Wissahickon terrane (Southwick, 1969) defined the dip of the prisms in the models. The use of shallower-dipping and northwest-dipping boundaries in the modeling did not yield good agreement between calculated and observed magnetic anomalies. In all cases the magnetic susceptibility was taken as the mean of all samples (291×10^{-5} emu/cm^3). While the Jenkins site had values below this and values at the other sites were larger, the standard deviations of the samples did not justify any differentiation of one location from another.

A series of profiles were constructed at right angles to the trend of the anomalies across and between the highest amplitude anomalies. Figure 8 shows four profiles across the pair of anomalies at the southwestern end of the mapped area (see Figure 6). Sections A-A' and B-B' across the western-most body show the existence of two steeply dipping slabs each approximately 90 m wide and extending to depths of 0.60 and 0.35 km on the south of the anomaly. A larger prism with a thickness of 0.65 km, a width of 0.77 km, and a length of 0.62 km is buried at a depth of 0.10 km.

Profiles C-C' and D-D' (Figure 8), across the body directly to the northeast, show a similar arrangement of a subequant prism (0.77 km thick x 0.77 km wide x 0.62 km long) with a steeply dipping slab 90 m wide x 0.55 km thick x 0.60 km

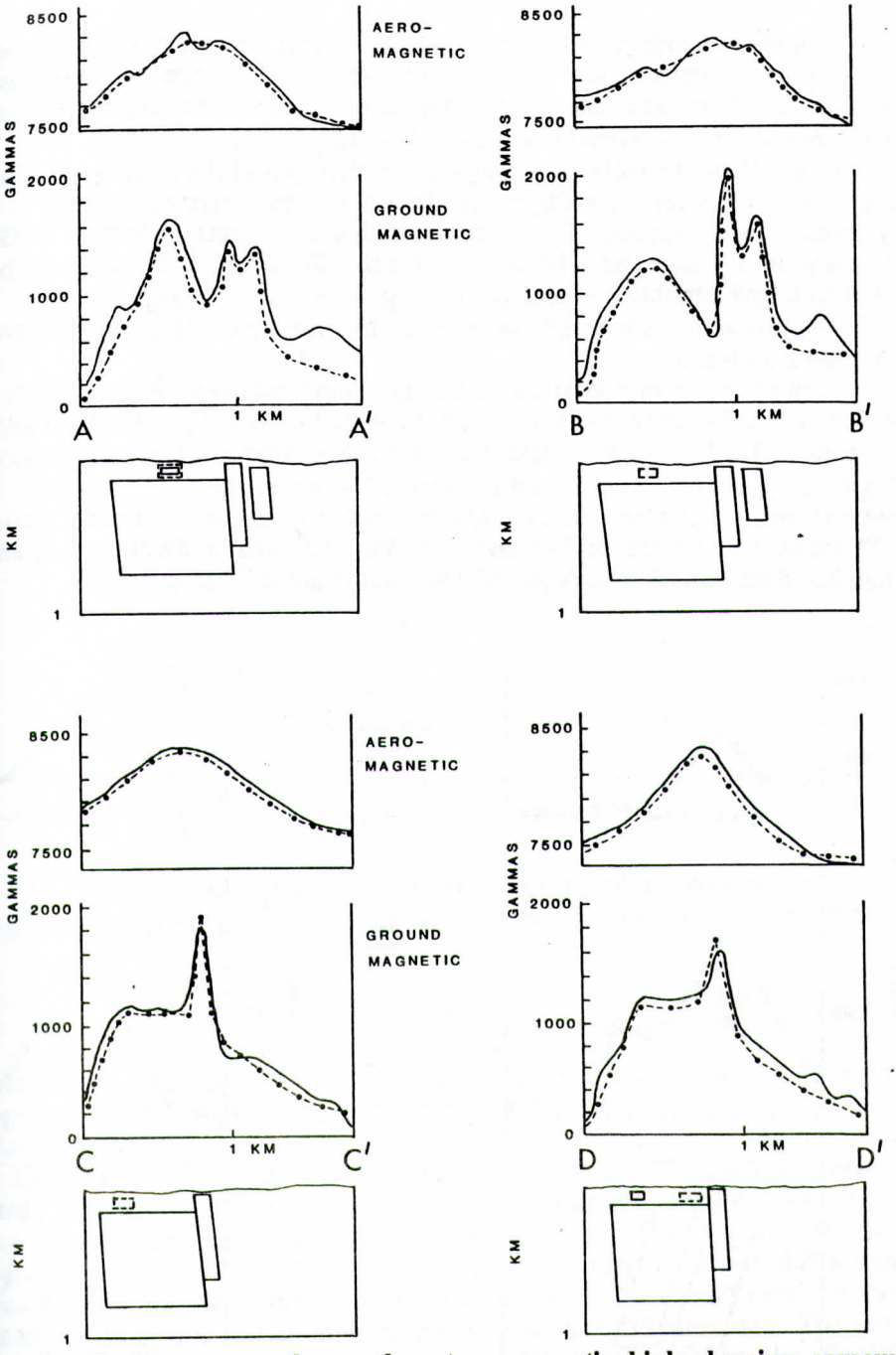

Figure 8. Profiles across the southwestern magnetic high showing agreement between calculated (dashed and dotted lines) and observed (solid lines) magnetic profiles for the aeromagnetic and ground magnetic data. Cross sections show the outlines of bodies which intersect the line of section (solid boundaries) and bodies which do not intersect the line of section (dashed boundaries).

long. Above the larger prisms, small tabular bodies were added to improve the fit between the calculated and observed curves. Such bodies are consistent with occurrences of isolated blocks and fragments of serpentinite in the schists of the Wissahickon terrane reported by others (Crowley, 1976; Southwick, 1969).

Figure 9 shows sections through the central part of the southwestern anomaly (see cross-section locations Figure 6). In this case the shape of the body is defined by three prisms dipping 75° southeast with an aggregate width of 0.95 km, a thickness of 1.8 km, and a length of 1.0 km. There is good agreement between calculated and observed values for both ground and aeromagnetic data. Again, some small near surface bodies were added to improve the fit for short wavelength anomalies on the map.

Further to the northeast the anomaly pattern narrows. Figure 10 shows the profile across the anomaly that lies on the state line between Maryland and Pennsylvania. The fit was evaluated only for the ground magnetic data since aeromagnetic data at the same resolution were not available from adjacent York County Pennsylvania. The steep, narrow anomaly is consistent with a nearly vertical slab 0.22 km across near the surface and widening somewhat at depth to 0.30 km. The modeled slabs extend to a depth of 1.8 km and are 1.0 km in length.

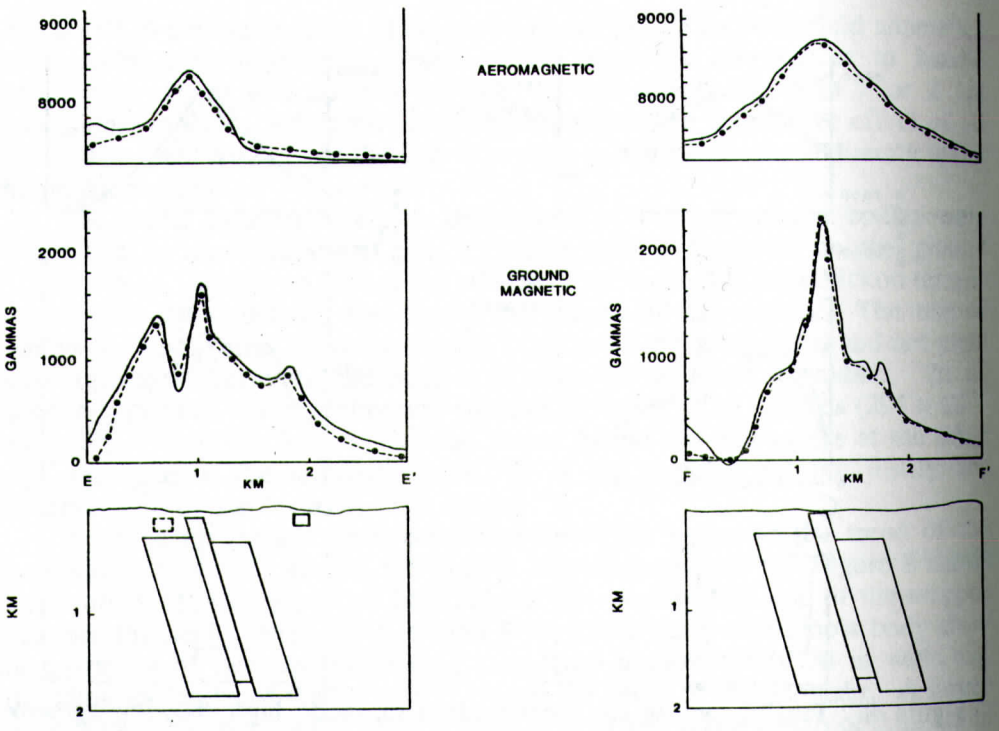

Figure 9. Profiles across the central magnetic high show agreement between calculated (dashed and dotted lines) and observed (solid lines) magnetic profiles. Cross sections show the outlines of bodies which intersect the line of section (solid boundaries) and bodies which do not intersect the line of section (dashed boundaries).

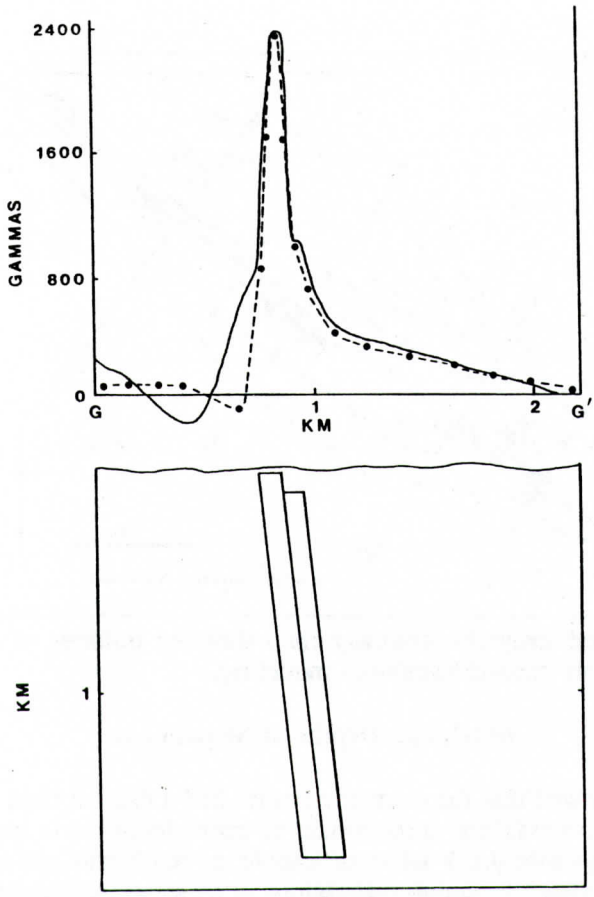

Figure 10. Profile across the northwestern magnetic high showing the match between the calculated (dashed and dotted) and observed (solid) ground magnetic data.

Map Outlines

Map outlines (Figure 11) were located by modeling a number of additional profiles across the trend of the bodies but between the major anomalies to check for consistency. These profiles show the cumulative effect of all of the slabs and prisms far from the particular section. They consistently showed good fits between calculated and measured anomalies. Figure 12, for instance, shows a good match between the measured and calculated magnetic values for a line of section in which no major serpentinite body occurs. The calculated map locations differ from previous map outlines at Cardiff-Whiteford (Southwick, 1969) and result in three new map positions for serpentinite at the Jenkins site (Figure 13). The clear separation between the continuous magnetic low northwest of the Cardiff-Whiteford area and the low northwest of the Jenkins area, supports the interpretation that there are two large, separate serpentinite bodies. Here the resolution provided by the ground survey allows improvement in modeling the sources of the magnetic anomalies.

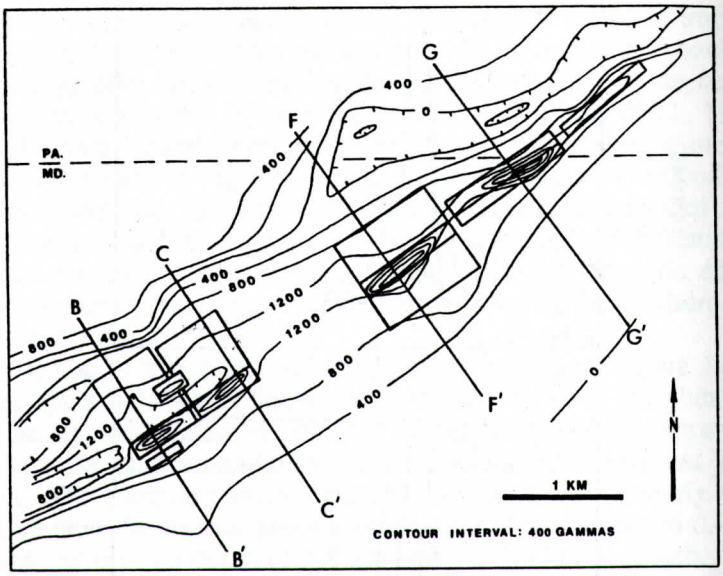

Figure 11. Ground magnetic anomaly map showing outlines of the serpentinite bodies derived from three-dimensional modeling.

Maximum Depths of Serpentinites

Modeling showed that the magnetic bodies had a distinct base at 0.8 to 1.8 km depth. Attempts to model the serpentinites to great depth led to broadening of the calculated anomalies beyond what is consistent with the wavelengths of the measured data. There is some uncertainty here as a function of the potential variation in susceptibilities and the sensitivity of the modeling equations themselves. We assess this uncertainty to be ±0.2 km for location of the lower boundary of the bodies. A second source of error in the location of this boundary involves changes in the susceptibilities of the serpentinite. If the ultramafic rocks are less serpentinized or contain less magnetite at depth for any reason, the bottom of the serpentinite bodies would be interpreted to extend to greater depths. We feel that this is unlikely, however, for the mean value we used in modeling is well within the range of serpentinites generally, and it would be just as likely that the susceptibilities would be higher as lower in different areas of the modeled bodies.

On the basis of the foregoing and with these uncertainties in mind, we also attempted to model the serpentinites beneath the western limb of the Peach Bottom fold assuming it has a synformal shape. Results show that highly magnetic serpentine bodies do not occur under the Peach Bottom structure but appear to terminate rather abruptly on the western limb. This relationship may lend support to the conclusion of Higgins (1972) that the Peach Bottom structure is anticlinal.

DISCUSSION AND CONCLUSIONS

Mineralogy and Magnetic Susceptibility

Largely because of the extreme alteration of the peridotite precursor, the

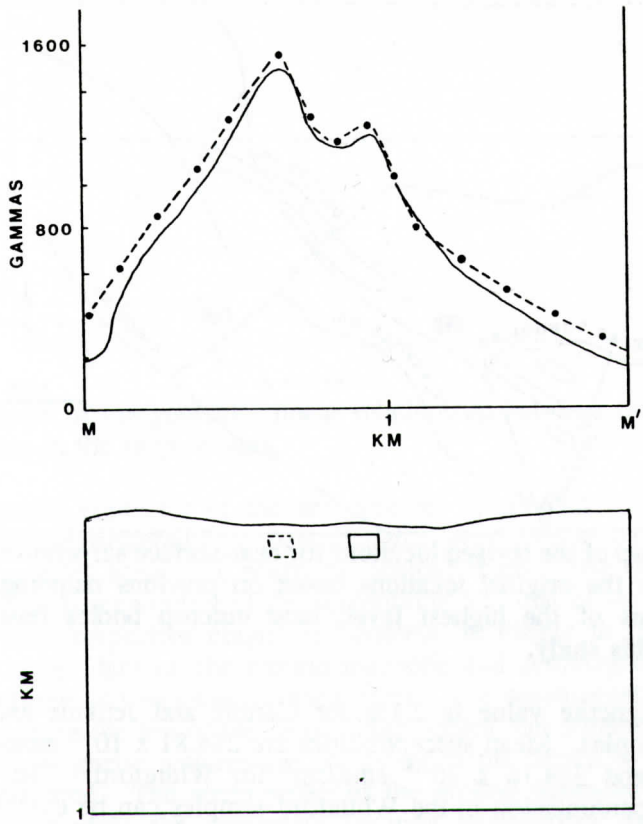

Figure 12. Profile of the area between the central and southwestern magnetic highs showing the match between ground magnetic data (solid line) and the calculated values (dashed and dotted line).

serpentinites of this study have strong magnetic signatures directly related to the magnetite content of the ultramafic rocks in relation to that of the surrounding schist. Less iron is admitted into the structure of the serpentine and associated magnesian secondary minerals than occurs within the olivine and orthopyroxene of the ultramafic protolith (Moody, 1976; Wicks and Whittaker, 1977). Thus, during the serpentinization process, the iron released from the olivine and enstatite forms tiny, discrete grains of magnetite. In the rocks studied, magnetite occurs as fine dust of this origin and also as coarser grains formed during late stages of serpentinization (Saad, 1969; Coleman, 1971). The relatively large amount of magnetite in the serpentinite is responsible for the substantial contrast in magnetic susceptibility between it and the country rock schist.

Previous studies have shown that susceptibility values correlate well with the extent of serpentinization (Saad, 1969; Thompson and Robinson, 1975; Honeycutt and others, 1981; Schiering and others, 1982; Hirt and others, 1987). However, for the northern Harford County serpentinites, the degree of serpentinization does not exhibit a linear relationship with magnetic susceptibility (Figure 14). The three Whiteford Quarry samples exhibit serpentine ranging from 32 to 52.5% in contrast to a range of 70.2 to 93% in the Cardiff and Jenkins samples. However,

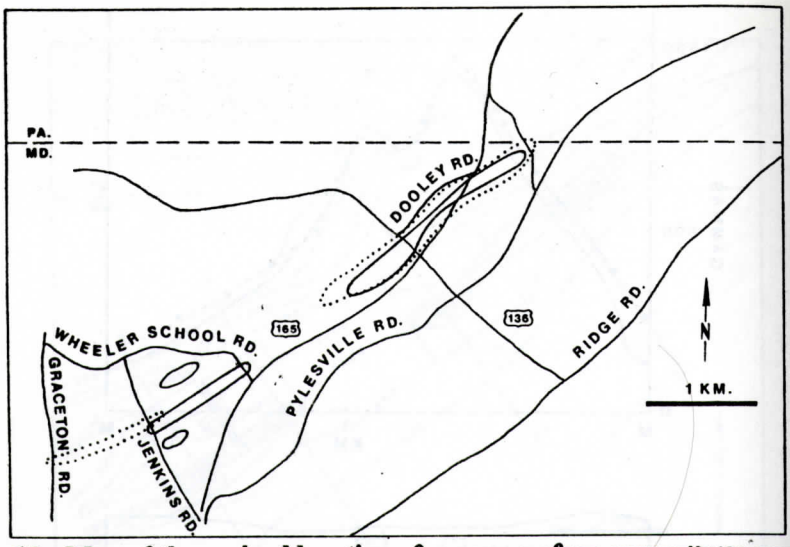

Figure 13. Map of the revised locations for near-surface serpentinite bodies. Dotted outlines show the original locations based on previous mapping. Solid outlines show locations of the highest level, near outcrop bodies based on magnetic modeling in this study.

the mean magnetite value is 2.1% for Cardiff and Jenkins and 2.9% for the Whiteford samples. Mean susceptibilities are 284.81 x 10^{-5} emu/cm^3 for Cardiff and Jenkins and 314.16 x 10^{-5} emu/cm^3 for Whiteford. The apparent lower degree of serpentinization in the Whiteford samples can be explained by the fact that some of the serpentine in them was later partially replaced by talc, as evidenced texturally in thin section. Susceptibility correlates with the degree of serpentinization, therefore, but is obscured in this study because of alteration of serpentine to talc in the Whiteford serpentinite. As shown in Figure 15, susceptibility correlates well with the abundance of coarse magnetite which was counted in the modes (Table 1).

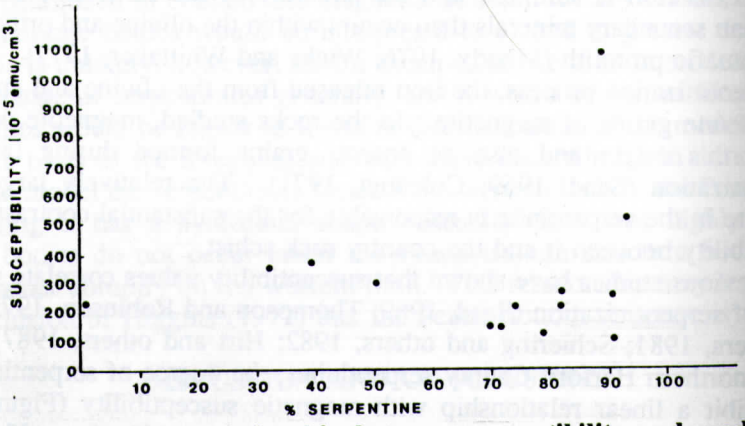

Figure 14. Graph of the relationship between susceptibility and modal percent serpentine in the area.

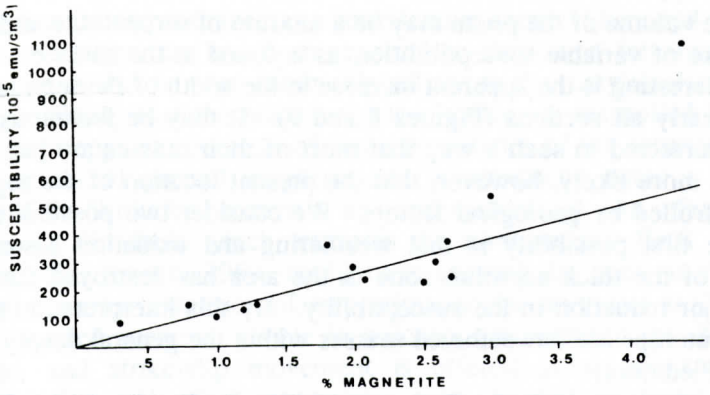

Figure 15. Graph of the generally linear relationship between susceptibility and modal magnetite in the serpentinites.

The magnetic character of the serpentinite, determined from petrographic study and magnetic susceptibility measurements, was used in calculation of the models from profiles across the magnetic contour maps. The extreme contrast between magnetic susceptibility of the serpentinite and that of the schist, a direct reflection of their respective magnetite contents, is visible in the well-defined positive anomaly evident on the ground magnetic and aeromagnetic maps. The two maps reinforce and supplement each other. The aeromagnetic data are less sensitive to depth to the top of the serpentinite bodies, but models matching both ground and aeromagnetic patterns are consistent in the depths to the bottoms of the bodies calculated. The steep peaks of the ground magnetic map allow for construction of models for accurately locating near-surface positions of the serpentinite.

Shapes and Boundaries of Serpentinites

The ultramafic bodies in this area have been mapped as a continuous layer of serpentinite (Cleaves and others, 1968; Southwick, 1969). This interpretation is consistent with the aeromagnetic data of Bromery and others (1964). The ground magnetic map and models presented here, however, show that these bodies exist as isolated, detached masses. The modeling has resulted in a better map location of the Cardiff-Whiteford body and three new locations of near-surface serpentinite bodies in the Jenkins area. The map outlines are narrow, but subsurface widths range from 150 and 220 m at Cardiff through 950 m at Whiteford to 770 m at Jenkins. The bodies dip steeply to the southeast and extend to depths ranging from 770 m at Jenkins to 1.8 km at Whiteford and Cardiff. The bodies are presented in plan view in Figure 13.

The prisms calculated are approximations of shapes of serpentinite which vary from a lenticular form at Cardiff to a blocky shape at the southern end near Whiteford. Although a thick body must be modeled at the Whiteford location to fit both ground magnetic and aeromagnetic measured data, the precise prismatic shape is meant only to indicate the region of higher magnetic susceptibility. The actual serpentinite bodies are likely to be much more irregular than is any modeled

prism, and the volume of the prism may be a mixture of serpentinite and schist and metagraywacke of variable susceptibilities, as is found at the surface.

More interesting is the apparent increase in the width of the serpentine bodies at depth in nearly all sections (Figures 8 and 9). It may be fortuitous that these bodies are intersected in such a way that most of their masses are just below the surface. It is more likely, however, that the present location of the tops of these bodies is controlled by geological factors. We consider two possibilities for this control. The first possibility is that weathering and oxidation associated with development of the thick saprolite zone in the area has destroyed the magnetite causing a major reduction in the susceptibility. By this interpretation the present serpentinite outcrops are unweathered masses within the general deeply weathered rocks of the Piedmont.

Saprolite thicknesses in the Piedmont of Maryland and northern Virginia are commonly 15 to 30 m and may exceed 50 m (Cleaves, 1968; Obermeier and Langer, 1986). Cleaves (1974) also demonstrates the destruction of magnetite in saprolites over mafic rocks and the common existence of gradational contacts between saprolite and unaltered crystalline rocks below. Costa and Cleaves (1984) have discussed lithologic and topographic controls of saprolite thickness in a general examination of the erosional history of the Piedmont in Maryland. They note that saprolite tends to be thickest in the rolling upland surfaces of the Piedmont such as in the area studied here.

Thus the existence of a thick saprolite which grades into the unweathered underlying rock may be a factor in the depths to the tops of the serpentinite bodies modeled in this study. The occurrence of isolated unaltered serpentinite fragments in structured saprolite (Cleaves, 1974) is consistent with the isolated serpentinite bodies modeled in the upper parts of the cross sections (Figures 8 and 9).

Nonetheless, the depths of saprolitization reported in the literature for the Piedmont of Maryland do not generally reach down to the 100 m determined for the tops of the serpentinites by the modeling in the southern part of the area. We consider the existence of saprolite cover as a partial control of the tops of the magnetic bodies, but we also consider an additional controlling factor.

The second possibility is that the serpentinite bodies in the southern part of the area occur within the schists of the Wissahickon terrane. Variation in depth to the top of the serpentinites may be a result of vertical movement along faults associated with those mapped by Southwick (1969) along the northwest margin of the serpentinite bodies and the Peach Bottom structure.

Lower Contacts of Serpentinites

Abrupt terminations at the base of the bodies may be the result of 1) mineralogical change to less serpentinized ultramafic rock at depth, 2) lithologic change to less mafic members of the ophiolite suite at depth, 3) faulting or shearing at the base, and/or 4) the inclusion of the serpentinites as rootless tectonic or sedimentary clasts within the schists.

It is possible that mineralogical or lithologic changes may be responsible for a sharp drop in susceptibility of ultramafic bodies. Such a change would almost certainly involve lesser serpentinization and fresher ultramafic or mafic rocks at depth. While large to moderately sized fragments of fresh or partly altered

peridotite or mafic associates are certainly not unknown in the Appalachians, most of these bodies are serpentinized to a considerable extent (Misra and Keller, 1978). Such serpentinization has not been reported to vary as a function of elevation within the bodies, but is more commonly related to the margins (Hess, 1933).

The possibility that the bottoms of the bodies are controlled by faulting is consistent with apparent controls of some boundaries of the serpentinites in plan view. Positions of ground magnetic and aeromagnetic contour lines indicate narrowing of the Whiteford section at its north-eastern end. An inferred northeast-trending strike-slip fault which transects the northwestern flank of the Peach Bottom fold (Southwick, 1969) could have sheared the body at Whiteford and displaced the narrow extension of serpentinite to the northeast at Cardiff (Figure 16). Slickensided surfaces, visible in outcrop, are evidence for shearing of the serpentinite, and strike-slip movement is offered as an explanation for the northeast-trending tail of a serpentinite mass located southeast of the area (Southwick, 1969). Further, the map and cross sections of Southwick and Owens (1968) offer the possibility that serpentinites, occurring as intrafault blocks within the fault zone, may be truncated by offshoots of the main strike-slip fault.

The orientation of the fault zone and steep dips of the enclosing schists parallel the orientation of the boundaries of the sides of the serpentinites. By this interpretation, the bodies may have been emplaced as fragments of a tectonically disrupted edge of a large ophiolite such as the Baltimore-State Line Complex.

The general parallelism between the long axes of the serpentinites and the foliation and outcrop pattern of the schists is also consistent with the emplacement of the serpentinites as blocks or slabs within a sedimentary mélange. The boundaries of the bodies may thus be clast margins against the finer grained matrix of metasedimentary rock. In places these margins may have been modified by chemical alterations and faulting. Modification of original boundaries by faulting is most obvious in the northeastern end of the area where modeling shows an extremely thin dipping slab. The shape of this slab appears too fragile to have been an unmodified sedimentary fragment. The subsequent deformations would surely have folded or otherwise have disrupted it. The location of this thin but extensive slab adjacent to the fault which truncates the Peach Bottom fold indicates considerable tectonic modification of the serpentinite bodies whatever their ultimate origin.

The shapes of most of the bodies support the view that the serpentinite bodies occur as clasts within a polygenetic mélange. The magnetic data also support the views of Southwick and Owens (1968) of faulting as a partial control for the boundaries of the serpentinites.

We cannot completely rule out the possibility of post-emplacement modification of Crowley's thrust-based serpentinites by the multiple deformations documented by Lapham and McKague (1964), and Higgins (1973). However, the shapes of the serpentinite fragments modeled in the area are typical of Appalachian ultramafic bodies (Chidester and Cady, 1972; Misra and Keller, 1978; Hatcher and others, 1984). The Wissahickon terrane has been described as a mass of chaotic clastic debris with a thickness of over 4.3 km (Crowley, 1976; Morgan, 1977) and it displays isolated masses of serpentinized rocks in many areas (Brown and Pavlides, 1981; Drake, 1985a). While the occurrence of both small fragments and the main ophiolite bodies in the Wissahickon terrane is certainly suggestive of a

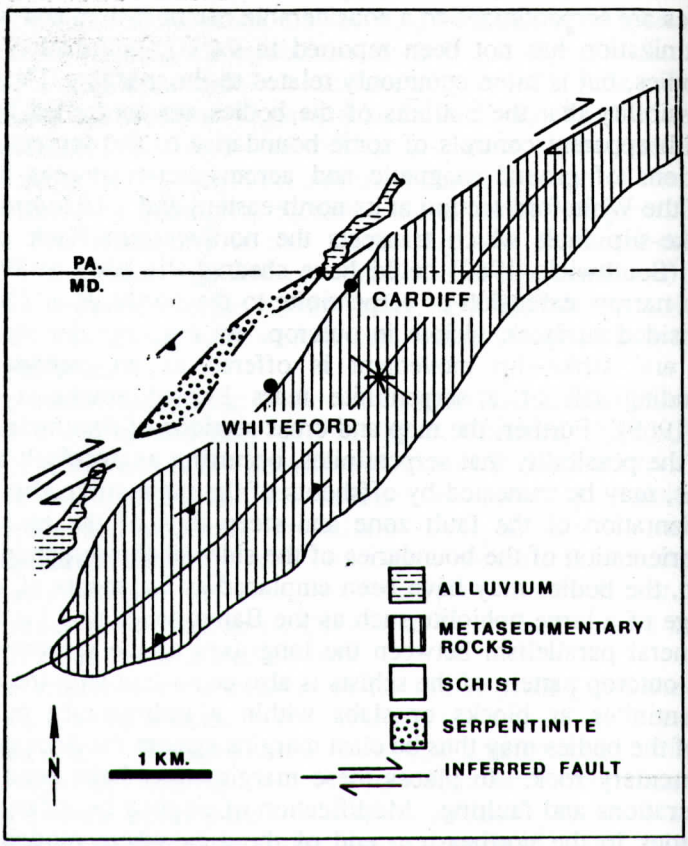

Figure 16. Generalized geologic map (after Southwick and Owens, 1968) showing the occurrence of serpentinized peridotite along the north side of the Peach Bottom fold with the inferred faulted boundary on the northwest.

common heritage for all the ultramafic rocks, the views of origin which arise from conflicting kinds of chemical data (Hatcher and others, 1984; Shaw and Wasserburg, 1984) and geological observations (many foregoing references) indicate that we should be wary in our conclusions.

Nonetheless, the geophysical models of the bodies of the western serpentinite belt are not consistent with simple models which connect them to the main mass of the Baltimore-State Line Complex. They are consistent with the development of a mélange associated with tectonic emplacement of a dismembered ophiolite.

ACKNOWLEDGEMENTS

We are pleased to acknowledge Sigma Xi, the Scientific Research Society, which contributed financial assistance for the study. Additionally, we are grateful to many people in Harford County, Maryland for their helpfulness and hospitality.

REFERENCES CITED

Bromery, R.W., Petty, A.J., and Smith, C.W., 1964, Aeromagnetic map of Bel Aire and Vicinity, Harford, Baltimore, and Cecil Counties, Maryland. U.S. Geol. Survey Geophysical Investigations map GP-482.

Bromery, R.W., 1968, Geological interpretation of aeromagnetic and gravity surveys of the northeastern end of the Baltimore-Washington Anticlinorium, Harford, Baltimore, and part of Carroll County, Maryland: Unpub. Ph.D. Dissertation, Johns Hopkins University, 124 p.

Brown, W.R., and Pavlides, Louis, 1981, Mélange terrane in the central Virginia Piedmont: Geological Society of America Abstracts with Programs, v. 13, no. 7, p. 419.

Chayes, F., 1956, Petrographic modal analysis: John Wiley and Sons, N.Y., 113 p.

Chidester, A.H., and Cady, W. M., 1972, Origin and emplacement of alpine-type ultramafic rocks: Nature of Physical Science, v. 240, p. 27-31.

Clark, W.B., 1898, Maryland Geological Survey, Volume 2, p. 32.

Clark, W.B., 1907, Geological map of Maryland: Maryland Geological Survey, Volume 6.

Cleaves, E.T., 1968, Piedmont and coastal plain geology along the Susquehanna aqueduct, Baltimore to Aberdeen, Maryland: Maryland Geological Survey Report of Investigations No. 8, 13 p.

Cleaves, E.T., Edwards, Jr., J., and Glaser, J.D., 1968, Geologic map of Maryland: Maryland Geological Survey.

Cleaves, E.T., 1974, Petrologic and chemical investigation of chemical weathering in mafic rocks, eastern Piedmont of Maryland: Maryland Geological Survey Report of Investigation No. 25, 28 p.

Coleman, R.G., 1971, Petrologic and geophysical nature of serpentinites: Geological Society of America Bulletin, v. 82, p. 897-918.

Coleman, R.G., and Keith, T.E., 1971, A chemical study of serpentinization - Burro Mountain, California: Journal of Petrology, v. 12, p. 311-328.

Condie, K.C., and Madison, J.A., 1969, Compositional and volume changes accompanying progressive serpentinization of dunites from the Webster-Addie ultramafic body, North Carolina: American Mineralogist, v. 54, p. 1173-1177.

Costa, J.E., and Cleaves, E.T., 1984, The Piedmont landscape of Maryland: a new look at an old problem: Earth Surface Processes and Landforms, v. 9, p. 59-74.

Crowley, W.P., 1976, The geology of the crystalline rocks near Baltimore and its bearing on the evolution of the eastern Maryland Piedmont: Maryland Geological Survey Report of Investigations No. 27, 40 p.

Dobrin, M.B., 1976, Introduction to geophysical prospecting: McGraw Hill Book Co., New York, 630 p.

Drake, Jr., A.A., 1985a, Sedimentary mélanges of the Central Appalachian Piedmont: Geological Society of America Abstracts with Programs, v. 17, no. 7, p. 566.

Drake, Jr., A.A., 1985b, Metamorphism in the Potomac Composite Terrane, Virginia-Maryland: Geological Society of America Abstracts with Programs,

v. 17, no. 7, p. 566.
Drake, Jr., A.A., and Morgan, B.A., 1981, The Piney Branch Complex - A metamorphosed fragment of the central Appalachian Ophiolite in Northern Virginia: American Journal of Science, v. 281, p. 484-508.
Fisher, G.W., Higgins, M.W., and Zietz, I., 1979, Geological interpretations of aeromagnetic maps of the crystalline rocks in the Appalachians, northern Virginia to New Jersey: Maryland Geological Survey Report of Investigations No. 32, 43 p.
Hatcher, Jr., R.D., Hooper, R.J., Petty, S.M., and Willis, J.D., 1984, Structure and chemical petrology of three southern Appalachian mafic-ultramafic complexes and their bearing upon the tectonics of emplacement and origin of Appalachian ultramafic bodies: American Journal of Science, v. 284, p. 484-506.
Hess, H.H., 1933, The problem of serpentinization and the origin of certain chrysotile asbestos, talc, and soapstone deposits: Economic Geology, v. 25, p. 634-657.
Higgins, M.W., 1973, Superimposition of folding in the Northeastern Maryland Piedmont, and its bearing on the history and tectonics of the central Appalachians: American Journal of Science, v. 273-A, p. 150-195.
Hirt, S.M., Heimlich, R.A., and Palmer, D.F., 1987, Geophysical study of a small ultramafic body near Newfound Gap, Buncombe County, North Carolina: Southeastern Geology, v. 27, p. 229-244.
Hjeldt, S.E., 1972, Magnetostatic anomalies of dipping prisms: Geoexploration, v. 10, p. 239-254.
Honeycutt, F.M., Heimlich, R.A., and Palmer, D.F., 1981, Magnetic survey of the Balsam Gap dunite, Jackson County, North Carolina: Southeastern Geology, v. 22, p. 223-231.
Hopson, C.A., 1964, The crystalline rocks of Howard and Montgomery Counties, *in* The Geology of Howard and Montgomery Counties, Maryland Geological Survey, p. 27-217.
Jahns, R.H., 1967, Serpentinites of the Roxbury district, Vermont, *in* Wyllie, P.J., ed., Ultramafic and Related Rocks: John Wiley and Sons, N.Y., p.137-155.
Johannsen, A., 1928, The serpentinites of Harford County, Maryland: Maryland Geological Survey, v. 12, p. 195-287.
Lapham, D.M., 1962, Northern Excursion Guidebook, International Mineralogical Association, p. 43-49.
Lapham, D.M., and McKague, H.L., 1964, Structural patterns associated with the serpentinites of southeastern Pennsylvania: Geological Society of America Bulletin, v. 75, p. 636-660.
Misra, K.C., and Keller, F.B., 1978, Ultramafic bodies in the southern Appalachians: a review: American Journal of Science, v. 278, p. 389-415.
Moody, J.B., 1976, Serpentinization: a review: Lithos, v. 9, p. 125-138.
Morgan, B.A., 1977, The Baltimore Complex, Maryland, Pennsylvania, and Virginia, in Coleman, R.G., and Irwin, W.P., eds., North American Ophiolites: Oregon Department of Geology and Mineral Industries Bulletin 95, p. 41-49.

Muller, Peter D., Candela, Philip A., and Wylie, Ann G., 1985, Liberty Complex: Polygenetic mélange in the Central Maryland Piedmont: Geological Society of America Abstracts with Programs, v. 17, no. 7, p. 671.

Muller, Peter D., and Edwards, Jonathan, Jr., 1985, Tectonostratigraphic Relationships in the Central Maryland Piedmont: Geological Society of America Abstracts with Programs, v. 17, no. 1, p. 55.

Obermeier, S.F., and Langer, W.H., 1986, Relationships between geology and engineering characteristics of soils and weathered rocks of Fairfax County and vicinity, Virginia: U.S. Geological Survey, Professional Paper 1344, 11 p.

Page, N.J., 1967, Serpentinization at Burro mountain, California: Contributions to Mineralogy and Petrology, v. 14, p. 321-342.

Pavlides, Louis, Arth, J.G., Daniels, D.L., and Stern, T.W., 1982, Island-Arc, Back-Arc, and m lange terranes of Northern Virginia; Tectonic, Temporal, and Regional Relationships: Geological Society of America Abstracts with Programs, v. 14, no. 7, p. 584.

Pavlides, Louis, 1985, Early Paleozoic Composite mélange terrane in the Central Appalachian Piedmont, Virginia and Maryland: Geological Society of America Abstracts with Programs, v. 17, no. 7, p. 686.

Pearre, N.C., and Heyl, A.V., 1960, Chromite and other mineral deposits in serpentine rocks of the Piedmont Upland, Maryland, Pennsylvania and Delaware: United States Geological Survey Bulletin 1082-K, p. 707-833.

Saad, A.H., 1969, Magnetic properties of ultramafic rocks from Red mountain, California: Geophysics, v. 34, p. 974-987.

Schiering, M.H., Heimlich, R.A., and Palmer, D.F., 1982, Radiometric and magnetic surveys of the Dark Ridge dunite, Jackson County, North Carolina: Southeastern Geology, v. 23, p. 89-98.

Shaw, H.F., and Wasserburg, G.J., 1984, Isotopic constraints on the origin of Appalachian mafic complexes: American Journal of Science, v. 284, p. 319-349.

Southwick, D.L., 1969, Crystalline rocks of Harford County, *in* The Geology of Harford County, Maryland: Maryland Geological Survey, p. 1-76.

Southwick, D.L., 1970, Structure and petrology of the Harford County part of the Baltimore-State Line Gabbro-Peridotite Complex in Fisher, G.J. and others, eds., Studies in Appalachian Geology: Central and Southern: Wiley Interscience, New York, p. 397-415.

Southwick, D.L., and Owens, J.P., 1968, Geologic map of Harford County: Maryland Geological Survey.

Telford, W.M., Geldart, L.P., Sheriff, R.E., and Keys, D.A., 1977, Applied geophysics: Cambridge University Press, New York, p. 105-217.

Thayer, T.P., 1967, Chemical and structural relations of ultramafic and feldspathic rocks in alpine intrusive complexes in T.J. Wylie, ed., Ultramafic and Related Rocks: John Wiley & Sons, New York, p. 222-239.

Thompson, G.A., and Robinson, R., 1975, Gravity and magnetic investigations of the Twin Sisters dunite, northern Washington: Geological Society of America Bulletin, v. 86, p. 1413-1422.

Wicks, F.J., and Whittaker, F.J.W., 1977, Serpentine textures and serpentinization: Canadian Mineralogist, v. 15, p. 459-488.

Williams, H., Turner, F.J., and Gilbert, C.M., 1982, Petrography: W.H. Freeman and Company, San Francisco, p. 535-536.

Zeitz, I., Gilbert, F.P., and Kirby, Jr., J.R., 1978, Aeromagnetic map of Maryland: U.S Geological Survey, Geophysical Investigations map GP-923.